1964

Modifications of the van Deemter equation in gas chromatography

Robert Morrison Bethea

Iowa State University

Recommended Citation

Bethea, Robert Morrison, "Modifications of the van Deemter equation in gas chromatography " (1964). *Retrospective Theses and Dissertations*. 3019.
https://lib.dr.iastate.edu/rtd/3019

BETHEA, Robert Morrison, 1935-
MODIFICATIONS OF THE VAN DEEMTER
EQUATION IN GAS CHROMATOGRAPHY.

Iowa State University of Science and Technology
Ph.D., 1964
Chemistry, analytical

University Microfilms, Inc., Ann Arbor, Michigan

MODIFICATIONS OF THE VAN DEEMTER EQUATION
IN GAS CHROMATOGRAPHY

by

Robert Morrison Bethea

A Dissertation Submitted to the
Graduate Faculty in Partial Fulfillment of
The Requirements for the Degree of
DOCTOR OF PHILOSOPHY

Major Subject: Chemical Engineering

Approved:

Signature was redacted for privacy.

In Charge of Major Work

Signature was redacted for privacy.

Head of Major Department

Signature was redacted for privacy.

Dean of Graduate College

Iowa State University
Of Science and Technology
Ames, Iowa

1964

TABLE OF CONTENTS

Page

NOMENCLATURE

A = constant in Equation 24, dimensionless

a = specific surface, $cm.^{-1}$

B = coefficient in Equation 24, dimensionless

B' = coefficient in Equation 27, $cm.ml./{}^{o}K^{3/2}$ min.

C = coefficient in Equation 24, dimensionless

C' = coefficient in Equation 27, ${}^{o}K^{3/2}$ min./cm.ml.

$C_{g,0}$ = solute concentration in the gas phase just before entering the colum, moles solute/mole of gas phase

$C_{g,r}$ = solute concentration in the gas phase in the rth plate, moles solute/mole of gas phase

$C_{\ell,r}$ = solute concentration in the liquid phase in the rth plate, moles solute/mole of liquid phase

C_{max} = solute concentration in the gas phase leaving the column corresponding to the appearance of the maximum peak height, moles solute/mole of gas phase

c = a constant

D_g = diffusivity of solute A in carrier gas B, $cm.^2$/sec.

D_ℓ = diffusivity of solute A in partitioning agent, $cm.^2$/sec.

d_g = gas film thickness, cm.

d_h = effective pore diameter, cm.

d_ℓ = effective thickness of liquid layer coating each particle, cm.

d_p = effective average particle diameter, cm.

E = coefficient in Equation 24, cm.$^{-2}$

E' = coefficient in Equation 27, $^oK^{3/2}$ min./cm.ml.

e = base of natural logarithms, 2.718...

F = volumetric carrier gas flow rate, ml./min.

G = coefficient in Equation 24, dimensionless

G' = coefficient in Equation 27, $^oK^{3/2}$ min./cm.ml.

H = height equivalent to a theoretical plate, cm.

j = function of ...

K = partition coefficient, moles solute/mole of liquid phase per moles solute/mole of gas phase

k = partition ratio, dimensionless

L = column length, cm.

M = molecular weight of partitioning agent, gm./gm. mole

N = total number of theoretical plates in a column, dimensionless

n = number of effective plate volumes in V^o, dimensionless

p = fraction of the total amount of solute in the liquid phase, dimensionless

Q_i = relative peak sharpness, dimensionless

q = fraction of the total amount of solute in the gas phase, dimensionless

R = multiple regression correlation coefficient, dimensionless

R_h = heating rate, ^{o}C/min.

R_{ij} = resolution between adjacent peaks, dimensionless

r = any plate, dimensionless

S_{ij} = relative separation between adjacent peaks, dimensionless

s = number of times a solute crosses the gas-liquid interface, dimensionless

T = absolute temperature, ^{o}K

t = temperature, ^{o}C

t_0 = starting temperature in LTP runs, ^{o}C

u = linear carrier gas velocity, cm./sec.

V = total volume of a phase in a column, cm.^{3}

V' = molar volume, cm.^{3}/gm.mole

V^o = gas volume entering the column in the time required for a solute to be eluted, cm.^{3}

V_R^o = retention volume of a solute, cm.^{3}

V_c = volume of unpacked column, cm.^{3}

V_s = volume of solids in a packed column, cm.^{3}

v = volume of a phase in the rth plate, $cm.^3$

v' = mean interstitial vapor velocity, cm./sec.

w = peak width measured between inflection tangent intercepts with the chart base line, min.

X = fractional column cross-sectional area, dimensionless

x = distance travelled by a solute molecule in the liquid phase, cm.

α = overall mass transfer resistance per unit volume of packing, $sec.^{-1}$

β = regression coefficient for the kth term in a regression model. The product of $\beta_i X_i$ is always cm.

γ = constant in the van Deemter equation accounting for the tortuosity of gas flow paths, $sec.^2$/cm.

δ = function defined by Equation 35

θ = retention time, min.

λ = constant in the van Deemter equation characteristic of the packing, dimensionless

μ = viscosity, gm./cm.sec.

π = 3.1416, dimensionless

ρ = correlation coefficient, dimensionless

σ = standard deviation, min.

ϕ_i = duration of initial constant temperature portion of an RFTP run, min.

ω = constant in the eddy diffusion expression of Giddings and Robison, dimensionless

Subscripts

A = solute

B = carrier gas

g = bulk gas phase

h = gas in pores

i,j = any sample components

k = any term in a regression equation

ℓ = substrate

p = solid support particles

I = gas phase in van Deemter's development

II = liquid phase in van Deemter's development

1 = different constants or functions

2 = different constants or functions

3 = different constants or functions

4 = different constants or functions

INTRODUCTION

Gas chromatography is a method by which the components of mixtures of volatile compounds can be separated. Although it is now used routinely for a diversity of applications from analyzing air pollutants in the parts per billion range to quality control of common industrial organic chemicals in the parts per thousand range to the preparation of 100 gram lots of some fine chemicals and drugs, the effects of different operating conditions are not yet understood.

The problem of determining the physical mechanism is quite fascinating and even more complex. The chromatographic process involves the flow of a multicomponent vapor phase through a packed bed of internally porous particles which are non-uniformly coated with a liquid phase. The vapor phase is subjected to the combined effects of simultaneous transport in at least two directions (axial and longitudinal) and the transfer of mass from one phase to the other. Neither of these effects is well understood even under greatly simplified conditions.

It was the purpose of this study to develop a mathematical relationship that could be used to predict the effect of temperature and flow rate changes on the efficiency of operation of a gas-liquid chromatographic column used to separate a known mixture of eight mono-nitroparaffins and to compare the effectiveness of the mathematical model developed here with similar models proposed by other researchers.

The experimental work was performed in three different series. In the first series, the temperature of the chromatographic column was held constant throughout the run (the CT series). In the second series, the column air bath temperature was programmed to increase linearly with time at several different rates from a constant initial starting point. This was the LTP series. In the last series, the column air bath temperature was programmed to remain at some fixed constant temperature level for different predetermined times and then to increase linearly with time at different heating rates. This method of operation is called ramp-function temperature programming (RFTP).

The basic apparatus needed for a gas-liquid chromatography system are shown as Figure 1. An inert carrier gas flows from the source on the left through a two stage pressure regulator to the column inlet. The sample to be analyzed is injected into the sample injection port as shown where the sample is vaporized and swept into the column by the carrier gas. The effluent from the column passes

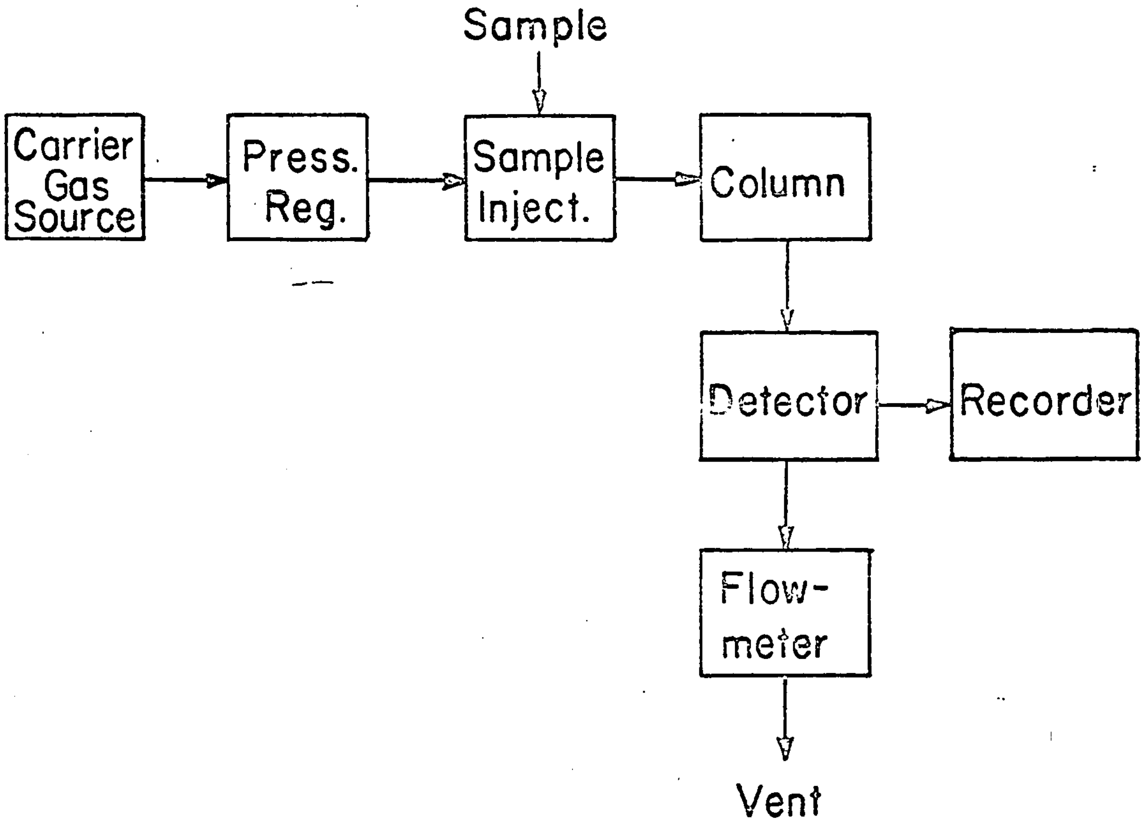

Figure 1. Block schematic diagram of apparatus for gas-liquid chromatography

directly to the detector where the different sample components are measured as they emerge from the column. The detector output is transmitted to a recorder to produce a permanent record of the separation accomplished. The effluent flow rate is measured by a flowmeter and is then vented to a hood.

Gas-liquid chromatographic analysis depends on the separation obtained when a complex organic mixture is passed in the vapor phase through a packed absorption column. The packing consists of a high boiling organic liquid partitioning agent (or substrate) which is supported in a thin layer on a finely divided inert solid such as crushed and sized firebrick. The purpose of the solid is to support the substrate and to provide a large area for mass transfer. The various components of the sample are separated because of differences in their respective absorption isotherms. The sample passes through the column in an ever widening band which is carried along by a continuous stream of eluting gas. The component which is least absorbed becomes more concentrated near the leading edge of the band while the component which is most absorbed becomes more concentrated near the trailing edge.

The degree of separation possible between any two compounds is determined by their partition coefficient, which is, in effect, an equilibrium constant. The partition coefficient K is the ratio of the solute concentration in the liquid phase to the solute concentration in the vapor phase at equilibrium. The partition coefficient is dependent upon such column operating parameters as temperature, vapor pressure, void fraction, liquid film thickness, etc.

After the sample is resolved into its individual components by the chromatographic column, the concentration of each component in the carrier gas can be measured by a thermal conductivity cell. The filaments of the cell are arranged in the form of a Wheatstone bridge: one pair of filaments form the measuring arm; the other pair form the reference arm. After the cell has been balanced, the presence of any compound in the measuring arm other than the carrier gas produces an electrical unbalance which is proportional to the concentration and which can be recorded in millivolts by a recording potentiometer. The curve obtained by plotting concentration or potential difference against time is referred to as an elution curve. The area under the curve is proportional to the concentration of the component in the sample.

The various components of a mixture can be identified because each is retained for a different length of time in the column. In other words, each substance has an unique retention time for a specific set of operating conditions.

PREVIOUS WORK

There have been almost 100 papers published in the last two years which are related to the study reported here. Only those articles have been cited which have a direct bearing on this work. The reader desiring a comprehensive review of the work done and in progress in the general area of mathematical treatment of different aspects of gas chromatographic theory should consult the texts by Dal Nogare and Juvet (8), Keulemans (19), and Littlewood (22) and the review articles on chromatographic theory and practice appearing in Analytical Chemistry each April.

The importance of solute diffusion effects in both the vapor and liquid phases on the spreading of a solute band is generally accepted. The diffusion of a solute in a gas is usually several orders of magnitude greater than the diffusion rate of that solute in a liquid. This is particularly true at high flow rates, i.e. at carrier gas flow rates greater than about 20 cc./min. measured at standard conditions. At very low flow rates, gas diffusion appears to be the limiting factor on efficiency of separation while at high flow rates, the limiting factor appears to be the rate of diffusion of the solute in the liquid phase.

A number of workers have derived equations relating column performance as measured by the HETP, or height equivalent to a theoretical plate, to different physical regions of a packed gas-liquid chromatographic column. The work of van Deemter *et al.* (9), Klinkenberg and Sjenitzer (21), Jones (17), Bethea and Adams (3) and others will be discussed after the statistical basis upon which HETP is based.

The nomenclature symbols used below and in subsequent equations have been changed in some cases from those originally used so that the various contributions of different authors may be more readily compared. The symbolism used here conforms to that presented in the initial section of this thesis.

Statistical Basis of HETP

Ideally, a small sample which is injected into a column and vaporized immediately should traverse the column with very sharp, well defined edges. Actually, this is not the case. Except for some relatively non-absorbed gases such as hydrogen, helium, etc., all compounds diffuse ahead of the main sample band. This is called leading. Similarly, because of equilibrium effects and absorption effects as yet not fully explained, all compounds exhibit some tailing. Tailing occurs when some portion of the solute is retained on the column material after the main solute band has passed by and is then slowly desorbed. If the amount of leading and tailing exhibited by a peak are equal, then the peak is said to be Gaussian in nature.

Glueckauf (15) pointed out that the behavior of solutes in a gas chromatographic column can be represented most accurately by a Poisson distribution. He also pointed out that if n, the number of "effective plate" gas volumes and r, the number of plates are sufficiently large, the Poisson distribution approaches a Gaussian distribution.

If the column can be considered as made up of r theoretical equilibrium stages or plates, and the solute is present in the rth plate, it will be distributed between the liquid and gas phases as K, the partition coefficient. The concentration of the solute in the liquid phase in the rth plate, $C_{\ell,r}$, will be related to the concentration in the gas phase in that some plate, $C_{g,r}$, as

$$C_{\ell,r} = KC_{g,r} \qquad (1)$$

Let the volumes of the vapor and liquid phases on the rth plate be v_g and v_ℓ, respectively. An incremental gas volume, dv, moving from the (r-1) plate to plate r carries with it an amount of solute $C_{g,r-1}$ dv. As the gas volume moves on to the r+1 plate, it will carry out an amount of solute $C_{g,r}$ dv. As a result of this vapor phase motion, the concentration of the vapor in the liquid and vapor phases of plate r are also changed. As the amount of solute transfer in the gas phase is the sole cause of the change in the amount of solute in plate r, the entire process can be expressed as the material balance given below as Equation 2.

$$(C_{g,r-1} - C_{g-r})dv = v_{\ell}\, dC_{\ell,r} + v_g\, dC_{g,r} \qquad (2)$$

Using Equation 1 to simplify Equation 2 and rearranging, the rate of change of C_g in the rth plate with respect to the gas volumetric flow rate is found as

$$\frac{dC_{g,r}}{dv} = \frac{C_{g,r-1} - C_{g,r}}{v_g + Kv_{\ell}} \qquad (3)$$

Keulemans (19) has given a solution to Equation 3 as

$$C_{g,r} = C_{g,0}\, n^r\, e^{-n}/r! \qquad (4)$$

where
$$n = V^{o}/(v_g + Kv_{\ell}) \qquad (5)$$

$C_{g,0}$ is the solute gas phase concentration just before entering the column. V^o is the quantity of gas which has entered the column by the time the leading edge of the gas phase reaches plate r. n is the number of "effective" or theoretical plate volumes in V^o. The effective plate volume is defined as the retention volume for a single theoretical plate.

The partition ratio for any solute is k which is related to p, the volume of solute in the liquid phase/total solute volume and q the volume of solute in the gas phase/total solute volume at any time for any segment of the column as

$$k = p/q \tag{6}$$

The partition coefficient K is related to k by

$$K = kV_g/V_\ell \tag{7}$$

where V_g and V_ℓ are the total volumes of gas and liquid in the column at any time, respectively.

The retention volume of any solute is V_R^o and corresponds to the volume of gas that has passed through the column between the time the sample was injected and the time of first appearance of the maximum peak height on the recorder. V_R^o is related to K by

$$V_R^o = V_g + KV_\ell \qquad (8a)$$

or

$$V_R^o = N(v_g + Kv_\ell) \qquad (8b)$$

where N is the total number of theoretical plates in the column. Using Equations 5, 8a, and 8b, n can be expressed as

$$n = (V^o/V_R^o)N \qquad (9)$$

The maximum solute concentration can be found from Equation 4 when n = r and $V^o = V_R^o$ as

$$C_{max} = C_{g,0}r^r e^{-r}/r! \qquad (10)$$

By setting r = N and making use of Sterlings approximation for exponentials,

$$C_{max} = C_{g,0}/(2\pi N)^{\frac{1}{2}} \qquad (11)$$

Inflection points for peaks as described by Equation 4 are found at $n = r \pm \sqrt{r}$ corresponding to volumes $V^o = V_R^o\ [1 \pm \sqrt{(1/N)}]$.

In a normal distribution tangents to the inflection points intercept the abscissa a distance 4σ apart where σ is the standard deviation of the distribution. As one standard deviation is $\theta_i/\sqrt{N}$. This leads at once to the basic relationship used in calculating the HETP from the number of theoretical plates, and L, the column length:

$$H = L/N = \frac{L}{16}\left(\frac{w_i}{\theta_i}\right)^2 \qquad (12)$$

The van Deemter Equation

The first really significant attempt to explain the mechanism of band broadening in gas chromatography was made by van Deemter _et_ _al_. (9) and Klinkenberg and Sjenitzer (21). These authors presented a rate theory in which HETP in packed gas chromatographic columns was related to the effects of three distinct phenomena on solute band spreading. The phenomena were the variation in the path length followed by any solute molecule due to the presence of multiply connected paths, channeling, etc.; molecular diffusion of the solute in the gas phase; and the resistance to mass transfer in the liquid phase. These authors considered each of these three phenomena as independent causes of band spreading. Thus, the variance of the solute distribution at any point within the column would be the sum of the variances associated with each phenomena.

Further examination of Equation 12 reveals that as

$w_i = 4\sigma$, $H = \sigma^2/L$ where σ^2 is the sum of all the variances of the different contributions to H.

In van Deemter's development, all mass transfer resistances are included in α, where α is the over-all mass transfer coefficient per unit volume of packing. In the development of their Equation 38

$$H = \frac{2D}{u} + \frac{2u\,X_g/\alpha}{(1 + KX_g/X_\ell)^2}$$

to their Equation 53,

$$H = \frac{2\gamma D_g}{u} + 2\lambda d_p + \frac{8d_\ell^2 KX_g u}{\pi^2(1 + KX_g/X_\ell)^2 D_\ell X_\ell}$$

it was assumed that mass transfer resistance in the gas phase may be neglected. The data for their system behave in accordance with this assumption. Resistance to mass transfer in the gas phase may not always be negligible, and the resistance to molecular diffusion in the pores of the packing particles may be significant, especially with low weight ratios of substrate to support as demonstrated by Golay (16).

The first or A term (also known as the eddy diffusion term) in the van Deemter equation was developed by Klinkenberg and Sjenitzer who showed that the variance in distance traveled by each solute molecule is proportional to a fraction of the thickness of a layer of particles of average diameter d_p through which the gas phase flows. It was their contention that this term is independent of the gas phase flow rate. Results published since this development have indicated that the A term is small (20), flow-dependent (15,20), and even negative (5). These results do not agree even for cases where the same type of solid support was used. Kieselbach (20) found that magnitude of the A term is an inverse function of the volume of the test sample and proposed that channeling might be the principal cause of the A term. His results indicated that this was the case for his particular system. In this respect, his results may be regarded as support for the original derivation of the van Deemter equation. It is felt that the principal result of channeling would be the production as asymmetric peaks because of the volumes offered for remixing of the solute components. A further cause of asymmetric peaks would be poor instrument design. In either case, asymmetric peaks are definitely non-gaussian in shape and so the assumptions of the van Deemter equation would be invalid.

Giddings and Robison (14) have recently reported on the failure of the eddy diffusion concept as expressed by term A of the van Deemter equation. They pointed out that velocity gradients may exist in packed columns in two regions: within a single channel between the particles and across the entire cross-section. These gradients are supposedly caused by one or both of two mechanisms: diffusion of the solutes from one flow path to another or by a solute molecule following a single randomly directed laminar streamline through the column. Here it must be noted that the classical eddy diffusion concept used by van Deemter et al. (9) and Klinkenberg and Sjenitzer (21) is based solely on the latter cause of velocity gradients while Golay's (16) theory of capillary column performance is based solely on the former source of velocity gradients. The data of Giddings and Robison support their contentions. To the author's present knowledge, no further work in this direction has been reported by any worker in the field of chromatographic theory.

The validity of the molecular diffusion, or B, term in the van Deemter equation has not been seriously attacked. van Deemter et al. (9) realized that although all solute molecules will spend the same average time Θ_g in the gas phase, this time will vary with the gas velocity. The variance in the elution curve so caused is then the product of the time a solute in the gas phase in the column and the molecular diffusivity of the solute in the gas phase.

Several groups of workers, notably Perrett and Purnell (24), Bohemen and Purnell (6, 7) and Jones (17) have all presented data to the effect that in many cases, for a wide range of solutes and substrates, the relatively slow molecular diffusion of solutes in the carrier gas is a significant cause of peak spreading. This might be expected as several of these workers have found that the Reynolds number based on superficial vapor velocity in the empty column and the average diameter of the packing particles is less than 1.

The validity of the C term in the van Deemter equation (the resistance to mass transfer in the liquid phase) has never been questioned though it has been frequently misinterpreted. This term actually represents the combined resistances of the transfer of a solute molecule across gas-liquid interface and the slow molecular diffusion of the solute in the liquid phase. No known attempts have been made to separate this term into its proper steps.

van Deemter _et_ _al_. (9) considered the total variance in the distance traveled by a solute molecule between phase transfers as $\sigma^2 = s\ell^2$ where s is the number of times the solute crosses the gas-liquid interface and ℓ is the axial distance traveled in the phase between such crossings. The number of crossings is found by dividing the total time spent by the solute in the gas phase by the time needed to diffuse to and from the gas-liquid interface. The time spent by a sample molecule in the liquid phase $\theta_\ell = kL/u$. The time required for a solute molecule to diffuse from any point in the liquid layer surrounding each packing particle to the interface is proportional to d_ℓ^2/D_ℓ where d_ℓ is the liquid film thickness and D_ℓ is the diffusivity of the solute in the liquid.

The number of interface crossings is thus

$$s = (D_\ell/d_\ell^2)kL/u \qquad (13)$$

The distance between crossings is the product of the time per crossing and the velocity of the phase with respect to the solute. The distance a solute molecule travels in the liquid phase is then given by

$$\ell = d_\ell^2 u/D_\ell(1 + k) \qquad (14)$$

and the variance in the elution curve (chromatogram) is given by $kLd_\ell u/D_\ell(1 + k)^2$.

Jones' Modification of the van Deemter Equation

Jones (17) modified the original van Deemter equation to include terms for the resistance to mass transfer in the vapor phase, the effects of velocity gradients in the column (the validity of which has been shown by Giddings and Robison), and a term representing the interaction between these first two terms. Those desiring to follow the details of Jones' statistical approach should consult the original article. Briefly, Jones determined that the variance in path length caused by the necessity of a solute molecule to diffuse through a phase and across an interface is independent of all other sources of band broadening and could be therefore directly added to the other variances already discussed. He considered this variance to be equal to the number of such interface crossings times the gas phase diffusivity times the time required for a solute molecule to traverse the supposedly stagnant gas layer surrounding all surfaces of the packing particles. This added resistance to transport of the solute through the column is thus expressed as one of a sum of the variances which go to form the entire cause of band spreading and is represented as the fourth term of Jones' Equation 25 which is given below as

$$H = 2\lambda d_p + \frac{2\gamma D_g}{u} + \frac{c_2 k}{(1 + k)^2} \frac{d_f^2 u}{D_\ell} + \frac{c_2 k^2}{(1 + k)^2} \frac{d_g^2 u}{D_g}$$

$$+ c_3 d_p^2 u + 2\rho \sqrt{c_2 c_3} \frac{k}{1 + k} \frac{d_p d_g}{D_g} u$$

Jones also included as the fifth term of the equation given above a term representing the peak spreading due to the velocity gradients. He said that the velocity gradients should affect peak spreading in a manner proportional to the variance of the gas velocity. Giddings (12, 13) and Robison (14) have subsequently arrived at a new expression for the A term as given below which was discussed in the preceding section.

$$A = \frac{1}{\dfrac{1}{2\lambda d_p} + \dfrac{D_g}{\omega d_p^2 v'}}$$

where v' is the mean gas velocity in the interstices between the particles and ω is a constant characteristic of the packing.

Jones included the sixth term in his equation to account for the effects on solute band broadening caused by the fact that some solute molecules will stay close to the wall and will be greatly retarded because of the low velocity there while some other solute molecules will be in faster moving velocity zones. There does not seem to be any simple way to estimate values of ρ, the correlation coefficient between the gas phase mass transfer and the velocity gradient effects.

Modifications of Bethea and Adams to the van Deemter Equation

α is the overall mass transfer coefficient per unit volume of packing. α_I and α_{II} refer to the resistance to mass transfer in the vapor and liquid phases respectively. van Deemter's Equation 41 merely resolves $1/\alpha$ into what he considered its component parts as shown below. van Deemter's Equation 41 may be modified by substituting $\frac{1}{\alpha_g} + \frac{1}{\alpha_h}$ for $\frac{1}{\alpha_I}$. This separates the effects of resistance to diffusion in the bulk gas stream from the effects in the gas-filled, liquid-coated pores. This separation is necessary, as the gas in the pores is stagnant or at best in laminar flow. Thus diffusion in the pores would be entirely molecular in nature, because the relative magnitude of the mean free path of the solute molecules is very small compared with an average pore diameter of 0.4 to 2 microns. This range for pore diameter has been reported (2) for Johns-Manville red Chromosorb, which is similar to the crushed firebrick used as the solid support in this work. In the bulk gas phase, D in van Deemter's Equation 38 is the longitudinal dispersion coefficient and is a combination of molecular and eddy diffusivities, as shown in their Equation 53. No modification of α_{II} is necessary, since this term, representing the resistance to mass transfer in the liquid phase, will be the same mathematically regardless of the physical location of the liquid. The usual assumption may be made that the coating within the pores of the particles is of the same thickness as the substrate coating on the external particle surfaces. With this modification, van Deemter's Equation 41 becomes

$$\frac{1}{\alpha} = \frac{1}{\alpha_g} + \frac{1}{\alpha_h} + \frac{K}{\alpha_\ell}$$

where $\alpha_g = a_p k_g = \dfrac{25 D_g a_p^2}{6X_g} = \dfrac{150 D_g X_p^2}{d_p^2 X_g}$

This is similar to the correlation for laminar flow (10). For uniform spheres, the surface may be expressed as

$$a_p = 6X_p/d_p \tag{17}$$

For a unit volume of packing,

$$X_h + X_p + X_g + X_\ell = 1 \tag{18}$$

Assuming that the macropores may be represented as cylindrical capillaries,

$$\alpha_h = a_h k_g = \frac{25}{6} \left[\frac{4\ell + d_h}{\ell d_h}\right]^2 X_h^2 D_g \tag{19}$$

where the term in brackets is the specific surface of a cylinder with one end (that farthest from the external particle surface) closed. The substrate coats the inside surface and the bottom of the cylinders. The expression for k_g remains unchanged, as we are still dealing with mass transfer in a laminar fluid. The resistance to mass transfer in the liquid phase, α_ℓ, has been expressed by van Deemter in Equation 41 as

$$\alpha_{II} = \alpha_\ell = \frac{\pi^2 D_\ell X_\ell}{4 d_\ell^2}$$

Equation 41 may be rewritten as

$$\frac{1}{\alpha} = \frac{d_p^2 X_g}{150 D_g X_p^2} + \frac{6 X_g}{25 D_g [(4\ell + d_h) X_h / \ell d_h]^2} + \frac{4 d_\ell^2 K}{\pi^2 D_\ell X_\ell} \tag{20}$$

D, the longitudinal dispersion coefficient, may be expressed as

$$D = \gamma D_g + \lambda u d_p \tag{21}$$

the sum of the molecular and eddy diffusivities. Since

$$k = K \frac{X_g}{X_\ell} \tag{22}$$

van Deemter's Equation 38 may be rewritten as

$$H = 2\lambda d_p + \frac{2\gamma D_g}{u} + \frac{2uX_g^2 d_p^2}{(1+k)^2 150 D_g X_p^2} + \frac{(6X_g^2/25)\,(2u)\ell^2 d_h^2}{D_g(1+k)^2\,[4\ell + d_h]^2 X_h^2} + \frac{2uX_g 4d_\ell^2 k X_\ell}{(1+k)^2 \pi^2 D_\ell X_h} \tag{23}$$

or more simply as

$$H = Ad_p + \frac{BD_g}{u} + \frac{Cud_p^2}{(1+k)^2 D_g} + \frac{Eud_h^2}{D_g(1+k)^2} + \frac{Gud_\ell^2}{(1+k)^2 D_\ell} \tag{24}$$

The absolute column temperature at any time during a linear temperature programmed run may be expressed as

$$T = t_0 + R_h \theta_i + 273 \tag{25}$$

For the case of isothermal work, this reduces to $T = t_0 + 273$.

The molecular diffusivity of a solute in a carrier gas, D_g, can be expressed (25) as

$$D_g = j(T^{3/2}) \tag{26}$$

We may now rewrite Equation 10 as

$$\frac{L}{16}\left(\frac{w_i}{\theta_i}\right)^2 = A + \frac{B'}{F} T^{3/2} + \frac{C' d_p^2 F}{(1+k)^2 T^{3/2}} + \frac{E' d_h^2 F}{(1+k)^2 T^{3/2}} + \frac{G' d_\ell^2 k F}{(1+k)^2 D_\ell} \tag{27}$$

where the primed coefficients indicate that the flow rate conversion from linear to volumetric units has been made for the unprimed coefficients in Equation 24.

The first two terms of the right side of Equation 27 represent the contributions of eddy diffusion and molecular diffusion in the bulk gas phase. The next three terms represent, in order, the resistance to mass transfer due to diffusion in the interstitial space between particles, within the pores of the particles themselves, and in the liquid layer. Terms 3 and 4 actually describe the same mechanism, but each represents a different physical region where the resistance to mass transfer is applicable.

Significance of HETP

The performance of gas chromatographic columns, like that of fractional distillation columns, is often expressed in terms of the number of theoretical plates in the column or in the HETP corresponding to the given separation in a particular column. The definition of the theoretical plate is the same in both cases, but the number of theoretical plates required to perform a given separation is much greater in gas chromatography than in fractional distillation. The number of plates required in a chromatographic separation is about equal to the square of the number of plates required for that separation by fractional distillation. The reason for this large difference is simple. In chromatography, only that part of the column occupied by the solutes is effective in performing the separation. At any one time, only a small portion of the chromatographic column is in use. In distillation, all of the column is working all the time to separate the components of the mixture.

One frequent misconception should be immediately cleared up: HETP as applied to gas chromatography does not measure the height equivalent to a theoretical plate but represents more nearly (9) the height of an equilibrium transfer unit, or HTU, as frequently encountered in the literature dealing with absorption in packed beds. The HETP expression for column efficiency is a carry-over from distillation technology and has become so firmly entrenched in chromatographic literature that it seems impossible to change.

Another point to consider is the use of HETP as a criterion for measuring column performance in quantitative analysis. Consider the chromatogram presented as Figure 2 corresponding to the best isothermal separation obtained for the 8-component test mixture. HETP values for NM, 2-NP, and 1-NB are 0.157, 0.215, and 0.115 cm., respectively. If the HETP data were considered alone, one would be tempted to say that the column separated 1-NB more efficiently than either of the other two components. Examination of the chromatogram readily shows that this is not strictly true. The 1-NB peak leads badly, the NM peak tails slightly, and the 2-NP peak shows neither leading nor tailing. As HETP is calculated from retention time data and the corresponding recorder base-line intercept between tangents drawn to the inflection points on the sides of a peak, leading and tailing can greatly influence any calculated HETP by their effect on w_i. Thus a peak totally unsuitable for quantitative analysis such as 1-NB in Figure 2 can actually appear to have been

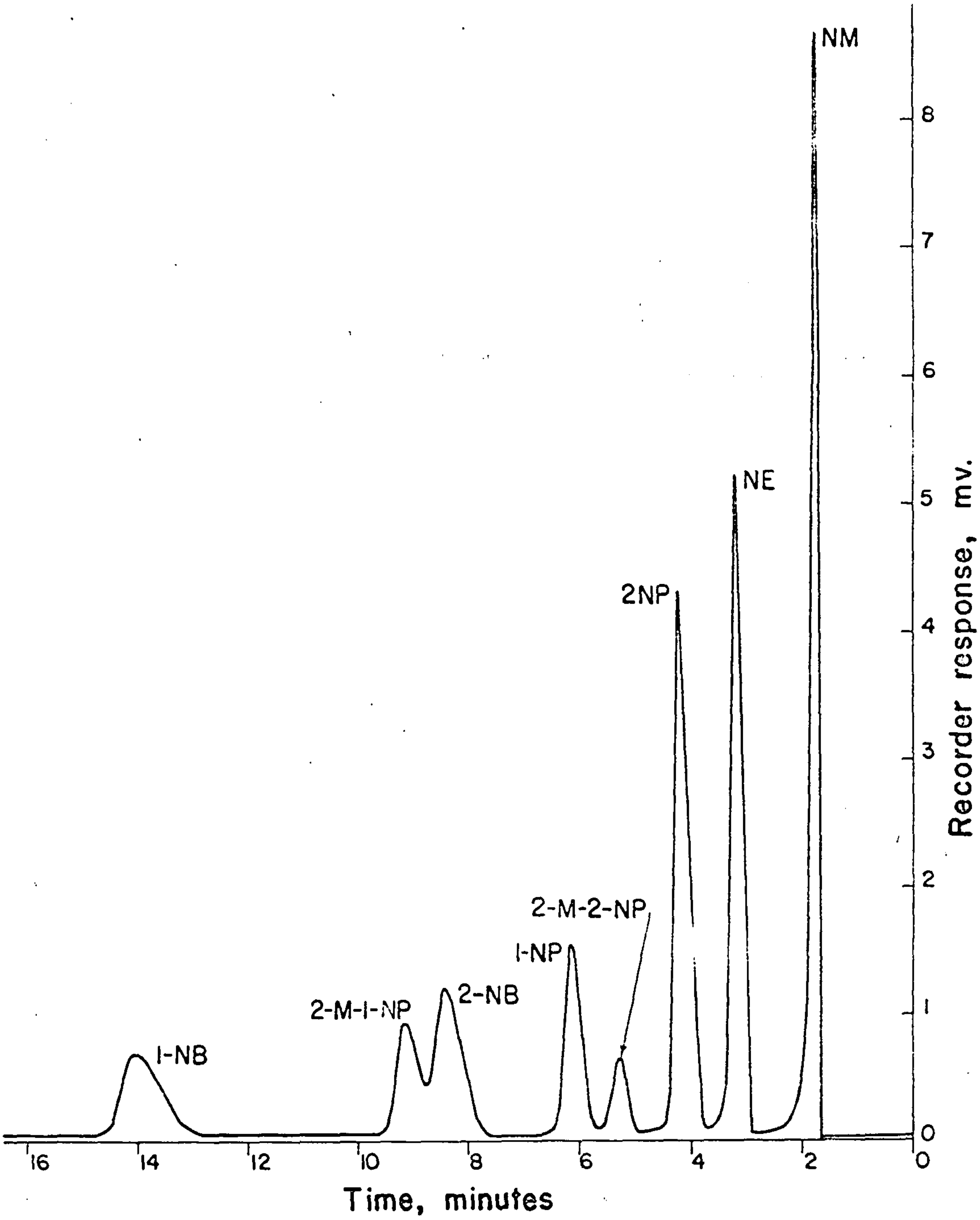

Figure 2. Optimum isothermal separation of the C_1 to C_4 nitroparaffins at 50°C and 90 ml. H_2/min.

more efficiently separated by the column than 2-NP. This usually occurs only when the substrate and the solute have widely differing polarities.

HETP does not give any direct information as to whether or not two peaks overlap. If they do, they are worthless for quantitative analysis. It can be used with retention time data to estimate such overlaps. HETP values for 2-M-1-NP and 2-NB are 0.086 and 0.115 cm., respectively. Here 1-NB and 2-NB have the same HETP yet 2-NB is almost half occluded by the 2-M-1-NP peak.

Although the HETP concept is not directly useful for quantitative analysis, it is a valid criterion (mis-named or not) for measuring column efficiency. Consider the research worker or practical gas chromatographic analyst who is trying to reproduce a chromatographic analysis system reported in the literature as being satisfactory for a given separation. Assume that (as is generally the case) a sample chromatogram has not been shown in the article but that the retention time and HETP have been given for each peak. The analyst reading such a report can tell immediately from the column length, retention times, and HETP values approximately how wide the peaks are. This gives him an idea as to how good the reported analysis technique really is. The proper use of such data can save many fruitless hours that might be wasted in an attempt to reproduce the reported analytical analysis system only to find that while the peaks are nicely separated in time, they are so broad as to make quantitative analysis impossible.

The author has found that the situation described above is quite common. In a recent attempt to obtain a satisfactory quantitative separation of the oxides of nitrogen, over 30 chromatographic systems reported in the literature as effective for this separation problem were investigated. The results were uniformly poor: no acceptable quantitative analyses were obtained even though some qualitative results were marginally acceptable. Only one of the more than 30 papers consulted in the course of that study showed a sample chromatogram. None gave HETP values. The only way to check the published results was to prepare the columns and attempt to get the reported separation, a time-consuming procedure. Had HETP values been given, it would have been possible to estimate the peak widths and thus the amount of peak overlap first. Depending on the results of such calculations, only those systems offering some promise of good, i.e. qualitative, separations would have been tested.

Many journals in the field of gas chromatography are now returning to their original copy requirements for analytical methods: show a sample chromatogram or give both θ_i and the corresponding HETP values. It is hoped that this practice will continue.

EXPERIMENTAL WORK

As stated earlier, the experimental work was carried out in three phases: constant temperature (CT), linear temperature programmed (LTP), and ramp-function programmed (RFTP) methods of operation. The test sample used in all this work was composed of the eight nitroparaffins listed in Table 1.

Apparatus

The unit used in this work was the F & M Scientific Corp. Model 500A programmed temperature gas chromatograph. The only modification made on this unit was the replacement of the soap film flowmeter by a Fischer and Porter rotameter, Flowrator tube No. 08-150/13 with stainless steel float, calibrated at operating conditions. No base line drift or changes in flow rate were observed during the linear programmed temperature runs. The sample injection port was maintained at 200°C for each run. Samples were injected through a self-sealing silicone rubber septum with a 10-μl. Hamilton microsyringe. The carrier gas used was hydrogen (extra dry grade, The Matheson Co.) which was dried before use by passing through a 12-inch length of 3/8-inch pipe filled with No. 5A Linde Molecular Sieves installed in the

Table 1. Nitroparaffin specifications

Nitroparaffin	No.	Symbol	Wt. % Major Constituent	Wt. % Minor Constituents	Wt. % in Test Sample
Nitromethane	1	NM	99.85	NE, 0.06; 2-NP, 0.09	19.60
Nitroethane	2	NE	99.7	2-NP, 0.3	19.31
2-Nitropropane	3	2-NP	99.9+	....	21.82
2-Methyl-2-nitropropane	4	2-M-2-NP	99.9	....	3.43
1-Nitropropane	5	1-NP	99.9	2-NB) 1-NB) 0.1	8.86
2-Nitrobutane	6	2-NB	99.9	....	11.52
2-Methyl-1-nitropropane	7	2-M-1-NP	99.82	....	6.65
1-Nitrobutane	8	1-NB	99.96	....	8.81

inlet line to the thermal conductivity cell. The flow rate through the reference side of the detector was maintained constant at 25 ml. of hydrogen per minute at 28°C.

The output signal from the detector was supplied to a 0- to 5-mv. Bristol Dynamaster potentiometer, Model 1PH-570. It was necessary to operate the unit at an attenuation of X2, which has the sole effect of halving the peak heights, to keep the peaks on the 10-inch recorder strip chart. The chart speed used was 30 inches per hour.

The column used throughout this study was a 6-foot length of 1/4-inch outside diameter copper refrigeration tubing coiled on a 3-inch mandrel after being filled with a 2 to 1 mixture by weight of Armeen SD (10 grams per 100 grams of inert support) and Apiezon N grease in the same proportion. The inert support used was the -48 + 65 Tyler standard screen fraction of crushed and sized Johns-Manville Type C-22 firebrick. The packings were prepared separately (9) and were mixed after preparation by dry screening several times on a 65-mesh Tyler screen. The screening has the additional advantage of removing any fines produced during the substrate impregnation step. The packings were heated in an oven with circulating air stream at 150°C for 24 hours before mixing.

The choice of this mixed packing was based on preliminary studies in this laboratory to determine the most suitable packing for the quantitative separation of nitroparaffins and the oxygenated compounds expected in the product stream from the vapor phase butane nitrator used by Adams (1).

Operating Conditions

Each series of the experimental work was designed and conducted as a randomized complete block experiment. In the CT series, blocking was done on flow rate levels and different constant temperature levels were used as the treatments. In the LTP series, the blocks were again the flow rate levels. This time the treatments were different linear heating rates. In the RFTP series, the durations of the initial $40^{\circ}C$ constant temperature period were used as treatments and the linear heating rate levels were used as blocks.

A minimum of two replicates were made at random for each set of conditions within each flow rate group for the CT and LTP phases using a 4 μl sample of the test mixture for each run. Additional replicates were made at random over the entire experiment. These additional runs showed that there was no change in column characteristics with time and that the experimental conditions and retention times of the nitroparaffins were reproducible with an experimental error of no more than ±0.8% over a six month period. The total number of CT and LTP runs were 73 and 78 respectively. The experimental conditions are shown in Table 2 for the CT and LTP work and in Table 3 for the RFTP work.

In all, a total of 106 runs were made in the RFTP series. A minimum of two replicates were made at each set of operating conditions shown in Table 3. In each case the average retention time for 1-NP corresponding to each set of experimental conditions is shown.

Summary of Previous Results

In the attempt to find system operating conditions suitable for use as a routine analytical method for the analysis of the nitroparaffins an $R_{ij} \geq 0.6$, corresponding to the resolution between adjacent peaks, was found by experiment to be a satisfactory column performance criterion. This was determined in the laboratory against seven widely differing known mixtures of the eight nitroparaffins.

Table 2. Retention times for 1-nitropropane and experimental conditions for determination of optimum operating conditions for maximum separation and resolution of nitroparaffins

	Flow rate$_2^a$ F, ml./min.			
	60	90	120	150
	Retention times, minutes[b]			
Temp., °C.	Constant temperature			
40	20.21	12.70	9.79	8.66
50	15.53	8.68	6.65	5.59
60	8.06	6.38	4.40	4.02
70	5.92	4.62	3.34	2.86
80	4.39	3.22	2.54	2.31
Heating rate °C./min.	Linear temperature programming[c]			
2.9	11.82	9.73	7.41	7.03
4.0	10.42	8.56	7.06	6.28
5.6	9.18	7.46	6.14	5.88
7.9	7.66	6.53	5.39	5.24
11.0	6.85	6.00	4.99	5.05
15.0	5.66	4.92	4.27	4.23

[a] Hydrogen flow rate measured at 28°C.

[b] Measured from injection point to appearance of peak maximum height

[c] Starting temperature, t_0 = 40°C.

Table 3. Retention times for 1-nitropropane and experimental conditions for determination of optimum operating conditions for maximum separation and resolution of nitroparaffins by ramp-function temperature programming

	Duration of initial constant temperature[a] period, min.						
	2	4	6	8	10	12	15
	Retention times, min.[b]						
Heating rate, °C/min.							
2.9	10.41	11.09	11.56	11.83	12.22	11.96	12.27
4.0	9.31	9.91	11.38	11.92	11.74	12.08	11.76
5.6	8.45	9.84	10.81	11.51	11.53	11.78	11.64
7.9	7.98	9.30	10.41	11.32	11.74	12.11	12.20
11.00	7.26	8.83	9.98	10.49	11.10	10.12	10.10
15.0	6.05	7.46	8.50	9.26	9.52	9.56	9.11

[a] t_0 = 40°C

[b] Measured from injection point to appearance of peak maximum height

R_{45}, corresponding to the resolution of 2-M-2-NP from 1-NP and R_{67}, corresponding to the resolution of 2-NB from 2-M-1-NP tested the experimental data most severely. R_{45} fell between 1.2 and 1.94 for the constant temperature data and between 0.8 and 1.72 for the LTP data. Since R_{67} is less than 0.8 for both sets of data, it was controlling as to the choice of operating method and conditions. For the CT series, the optimum value of R_{67}, 0.80, was found at 50°C and a hydrogen flow rate of 90 ml./min. A sample chromatogram obtained at these conditions is shown as Figure 2.

For the LTP series, a starting temperature of 40°C was found to be far enough above room temperature to allow rapid establishment of thermal equilibrium and yet low enough so that acceptable separations of both nitroparaffins and the C_1 to C_4 oxygenated compounds were obtained. The optimum R_{67} for the LTP series was found to be 0.64. This corresponded to a hydrogen flow rate of 60 ml./min. and a linear heating rate of 2.9°C/min. A typical chromatogram obtained under these conditions is shown as Figure 3. The primary advantage in using LTP was the production of more symmetrical and evenly spaced peaks than those obtained by CT analysis.

It was thought that a combination of CT and LTP opera-

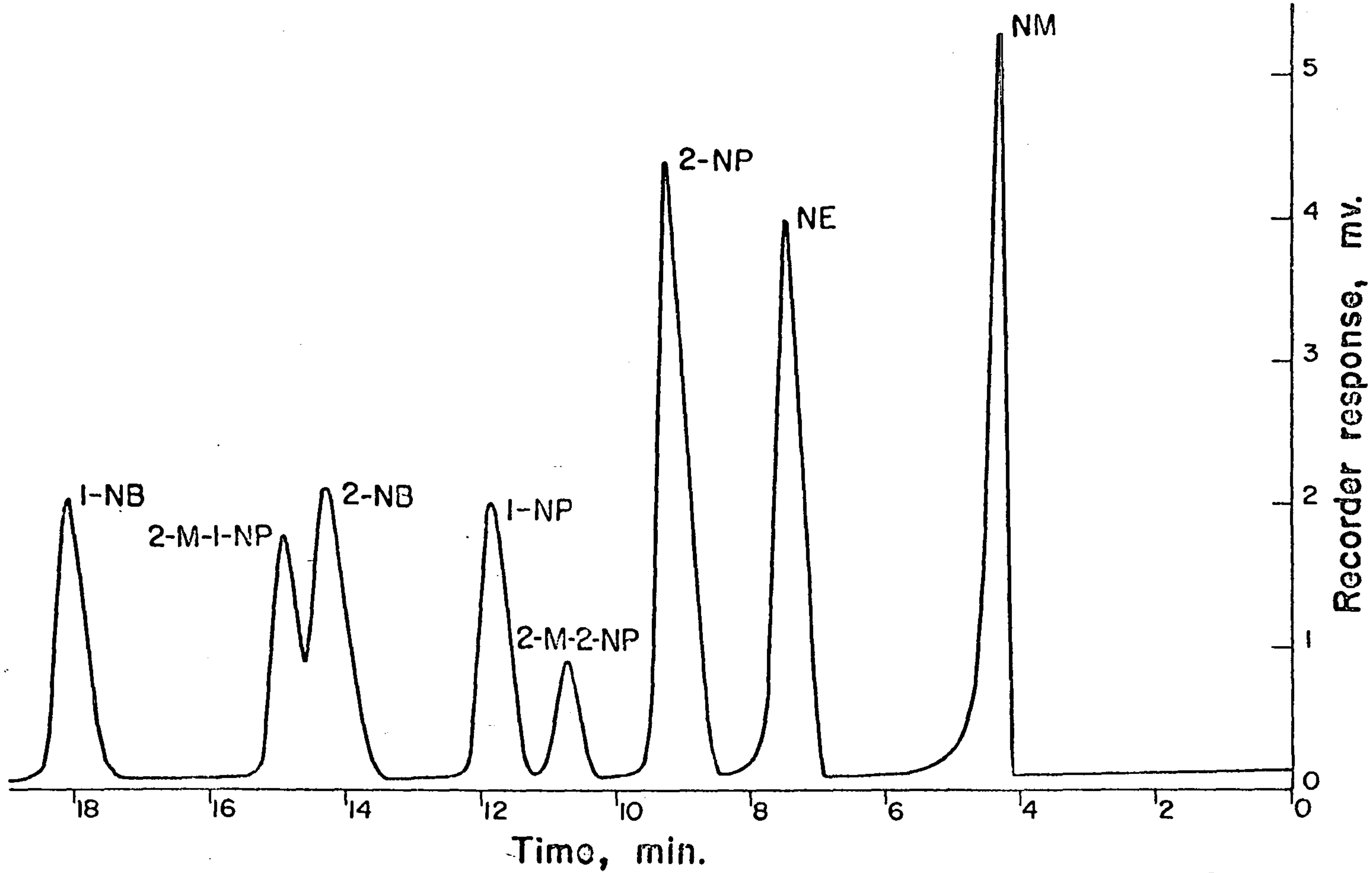

Figure 3. Optimum LTP separation of the C_1 to C_4 nitroparaffins as 2.9°C/min. (starting from 40° at time zero) and 60 ml.H_2/min.

tion would result in improving the separations between the pair 2-M-2-NP and 1-NP and the pair 2-NB and 2-M-1-NP. The use of RFTP allowed part of the analysis to be made at 40°C where there was no overlapping of the lower molecular weight nitroparaffin peaks with the peaks of the oxygenated compounds present in the nitrator product streams. The higher molecular weight nitroparaffins were initially retarded during the CT period of an RFTP run and were then speeded up and greatly sharpened by the change in their partition coefficients due to the higher temperature in the LTP portion of each run. The result was a chromatogram of evenly spaced sharp peaks as shown in Figure 4. The optimum operating conditions corresponded to a 10 min. period at 40°C followed by LTP at 11°C/min. at a hydrogen flow rate of 60 ml./min. Under those conditions, the errors in accuracy and precision of the quantitative analysis were no more than ±0.5% as determined from multiple replicate analysis of known, gravimetrically prepared nitroparaffin mixtures. At these optimum conditions, values of R_{45} and R_{67} were 1.80 and 0.73 respectively. It was thus found that the use of the RFTP analysis technique increased the value of R_{67} by almost 15%. The increase in analysis time was less than

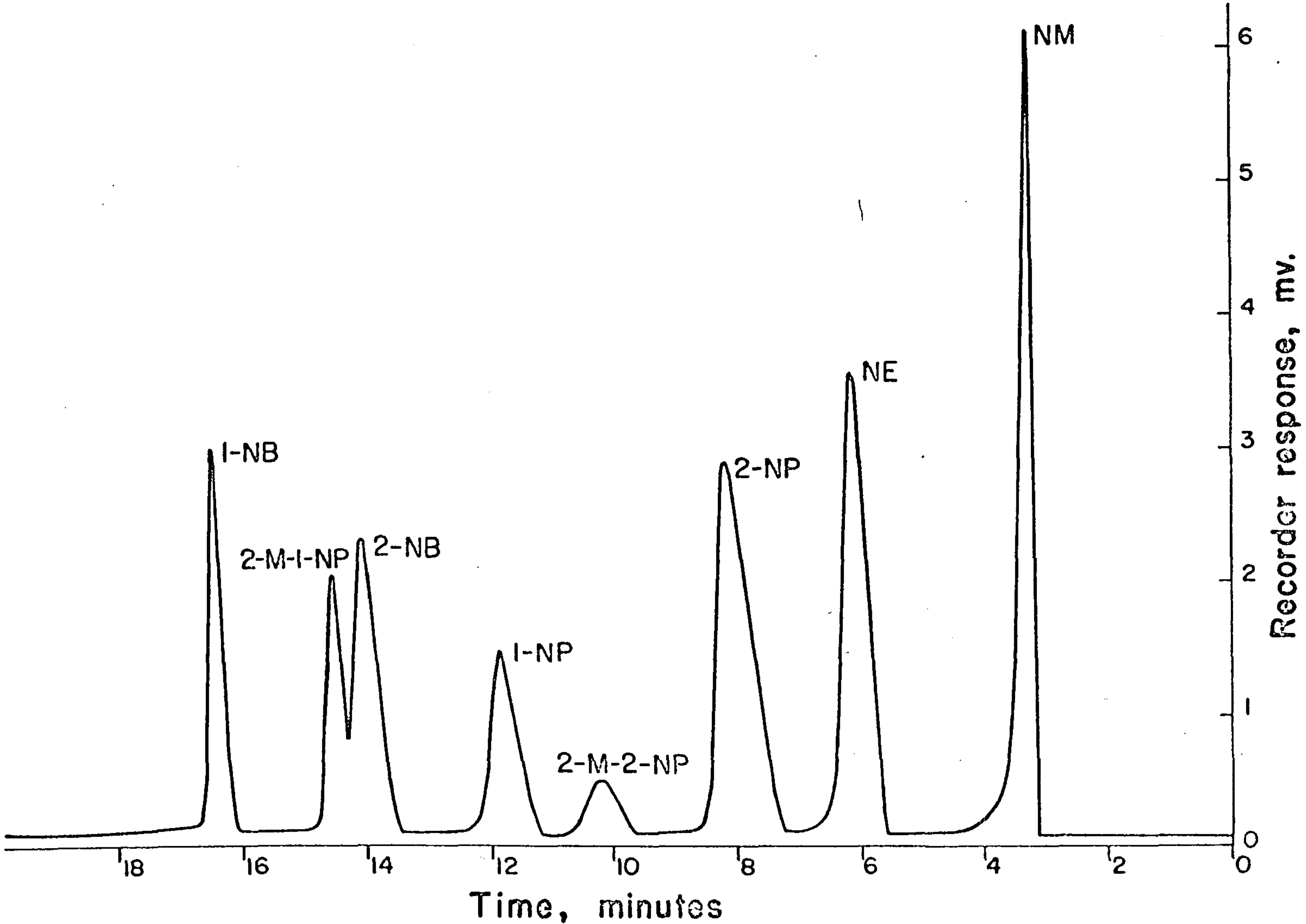

Figure 4. Optimum RFTP separation of the C_1 to C_4 nitroparaffins at 60 ml. H_2/min. and 40°C for 10 min. followed by LTP at 11°C/min.

2 min. as compared with the optimum CT and LTP conditions.

Although the use of RFTP provided an increase in the resolution of 2-NB from 2-M-1-NP, that operating technique was not used for routine analysis of the reaction products from the vapor-phase butane nitrator. There were two reasons for using the LTP mode of operation over the RFTP mode: no 2-M-1-NP was ever produced and the identification of the peaks in LTP operation was so simple that the nitration runs could be used as an experiment for senior students in the Chemical Engineering Department.

It was found that linear temperature programming of the Armeen SD-Apiezon N column at 2.9°C/min. starting from 40°C at a helium flow rate of 60 m./min. was effective in the separation of the C_1 to C_4 nitroparaffins; the lower molecular weight aldehydes, alcohols, and ketones; and water. A typical chromatogram of the nitroparaffins product so analyzed is shown as Figure 5.

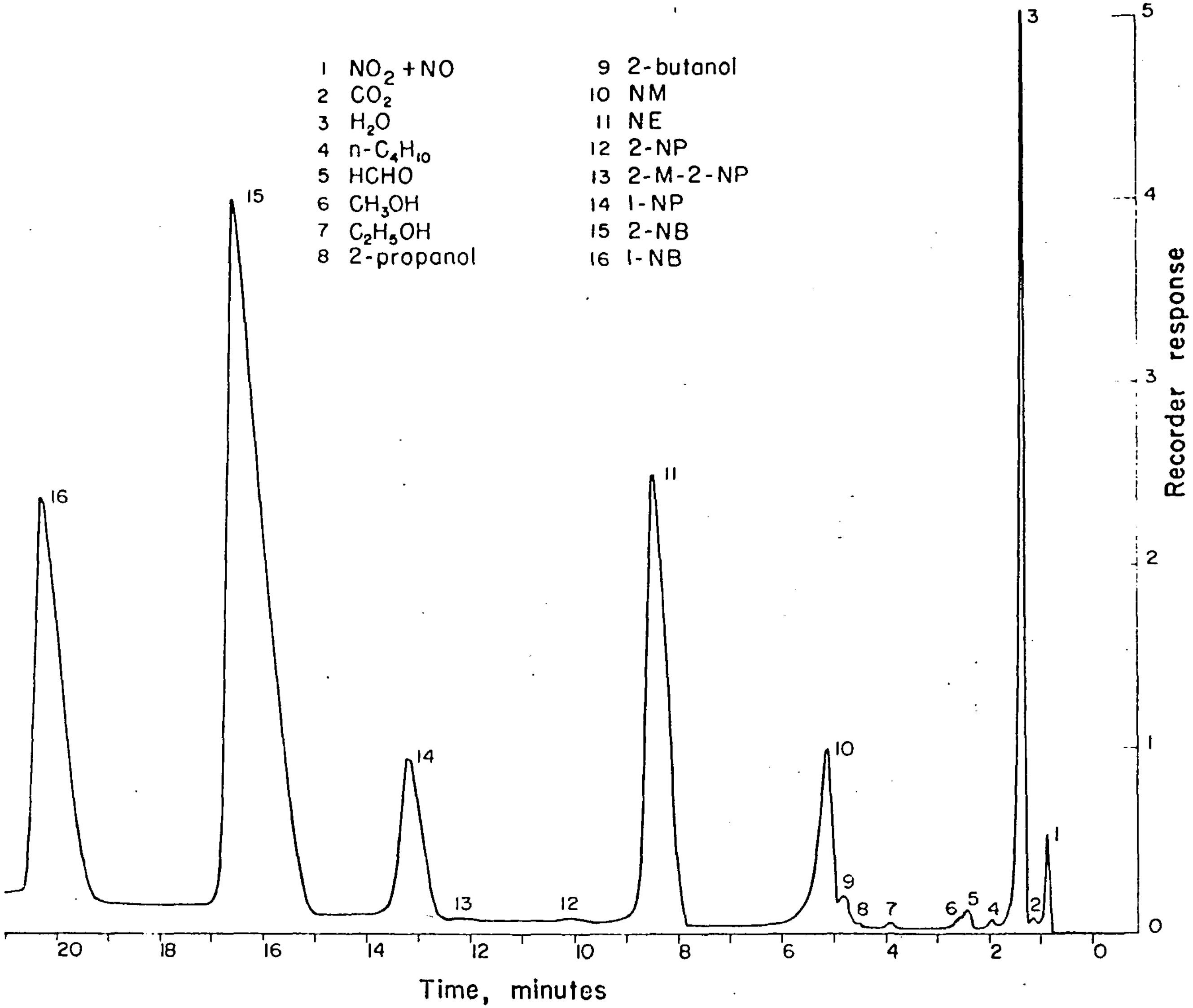

Figure 5. Typical chromatogram of the product from the vapor phase butane nitrator.

EXPERIMENTAL RESULTS

The primary purpose of the results reported here was to determine if the equation developed by Bethea and Adams (3) could be used to adequately express the effects of changes in heating rate, constant temperature level, flow rate, and duration of the initial CT period is an RFTP run on H, the height equivalent to a theoretical plate for the nitroparaffin system tested. The secondary purpose of the work reported here was to compare the correlations obtained by use of the Bethea-Adams equation with the Jones equation. A third reason for the experimental program was to attempt to resolve the question concerning the nature of the effects of the A term in the van Deemter equation.

Before any correlations could be made, certain calculations and estimates were necessary. The diffusivities of the nitroparaffins were calculated from the relationship given by Wilke and Chang (26)

$$D_{\ell} = \frac{7.4 \times 10^{-8} M^{1/2} T}{\mu \, (V')^{0.6}} \qquad (28)$$

Estimates of the molecular weights of Apizon N and Armeen SD were 2200 and 297 gm./gm.mole, respectively, as determined by the manufacturers. As the Apiezen N and Armeen SD were present in the packing in a weight ratio of 1 to 2, the molecular weight M of the mixed partitioning agent was estimated as 931.

The viscosity of the mixed substrate was determined experimentally with a Brookfield torsional viscometer over a wide temperature range. The experimentally determined relationship was

$$\log T = \log 426 - 0.0535 \log \mu \tag{29}$$

The values of the molar volumes, V', of the nitroparaffins were supplied by Commercial Solvents Corp. and are shown on Table 4. Also shown in Table 4 are the Antoine constants for the relationship between specific gravity and temperature for the nitroparaffins.

The values of K, the partition coefficient, were determined (8) from Equations 30 and 22.

$$K = \frac{\theta_i F - V_c}{V_s} \tag{30}$$

and was found to be

$$k = 0.89978\ \theta_i F - 19.606216 \tag{31}$$

The values of X_g and X_ℓ were determined from porosity measurements made on the untreated solid support and the finished column packing were 0.6512 and 0.1471, respectively.

Values of H were calculated from the chromatograms obtained in the experimental portion of this work and were fitted by multiple linear regression as outlined by Ostle (23, Chapters 8 and 9) to the following model

$$H = \beta_0 + \beta_1 X_1 + \beta_2 X_2 + \beta_3 X_3 \tag{32}$$

where

$$X_1 = T^{3/2}/F \tag{33a}$$

$$X_2 = F/(1 + k)^2 T^{3/2} \tag{33b}$$

$$X_3 = kF/(1 + k)^2 D_\ell \tag{33c}$$

and β_0, β_1, β_2, and β_3 correspond to A, B', $(C'd_p^2 + E'd_h^2)$, and $G'd^2$ in Equation 27. The β_i values were calculated using $d_p = 0.0252$ cm., corresponding to the average uncoated particle diameter; $d_h = 2\text{x}10^{-4}$cm. as estimated from the pore size and distribution data presented by Baker _et_ _al_. (2); and $d_\ell = 7.82 \times 10^{-6}$ cm. as determined from the weight of the substrate per gm. of solid support and the surface area of the solid support. The area of the solid support used in this study was determined as 4.18 $m.^2$/gm. as determined by

Table 4. Molar volumes and Antoine[a] constants for the mono-nitroparaffins

Compound	Molar volume cm.^{3}/gm.mole	A	B, 1/°C
NM	59.1366	1.1658	0.00138
NE	80.2086	1.0751	0.00122
2-NP	101.5756	1.0106	0.00111
2-M-2-NP	122.1565	0.9819	0.00106
1-NP	101.2075	1.0233	0.00109
2-NB	122.3312	0.9854	0.00100
2-M-1-NP	122.9299	0.9835	0.00100
1-NB	122.9037	0.9932	0.00099

[a] The specific gravity at t°c relative to water at 4°C, d_4^t is given by $d_4^t = A + Bt$

the Johns Manville Corp. by the Brunnaeur-Emmett-Teller nitrogen absorption method.

The regression coefficients tabulated in the Appendix in Table 12 from fitting the CT and the LTP data together to the model given by Equation 32. In Tables 13 and 14 are the regression coefficients obtained by fitting, respectively, the CT and LTP data separately to the model of Equation 32.

The RFTP data was fit to Equation 32 by rewriting Equation 25 as

$$T = t_0 + R_h \delta_i = 273 \qquad (34)$$

where

$$\delta_i = 0 \text{ for } \theta_i \leq \phi_i \qquad (35a)$$

$$\delta_i = \theta_i - \phi_i \text{ for } \theta_i > \phi_i \qquad (35b)$$

and ϕ_i is the duration of the initial 40°C period of an RFTP run. This in effect allowed only the LTP portion of an RFTP run to be fitted to Equation 32 as a check on the fit of the original LTP data. The regression coefficients resulting from this process are shown in Table 15.

Values of the multiple correlation coefficient, R, as determined by the Iowa State University Department of

Statistics Computation Center, representing the ability of an assumed regression model to fit or account for variations in the original data, are tabulated on Table 5. As seen on Table 5, the NM data are not very well accounted for by Equation 32 under any method of operation. The NE data were poorly fit for the constant temperature work, and the 1-NB data were even less well fit for the CT and CT + LTP work. With these exceptions, the value of R for any nitroparaffin is between 0.79 and 0.98 for all correlations. It is noted that the use of the RFTP data to check the original LTP data gives values of R somewhat higher for the RFTP than the LTP data with the exceptions of NM and 1-NB.

These data were also fit to Equation 32 without the β_0 term. The β_i values for these correlations are shown in Tables 16 to 19.

In some cases, (5, 9) the β_0 term is present in experimental curve fits; sometimes it is not. As the R values for NM were quite small for the direct fit of Equation 32, and since NM invariably appeared as a skewed (tailing) peak, it is thought that Kieselbach's (20) suggestion that the cause of the β_0 term is either due to component remixing in the dead volume of the column and sample side of the detector or to channeling or wall effects in the packing is correct. In either case, the peak asymmetry would increase with decreas-

Table 5. Values of R from the fitting of Equation 32

Compound	LTP + CT	CT	LTP	RFTP
NM	0.66842740	0.44680207	0.73282572	0.27678174
NE	0.81125771	0.47988884	0.86306467	0.86553656
2-NP	0.82497756	0.82885581	0.87624539	0.93444820
2-M-2-NP	0.84644933	0.79114215	0.85824353	0.91005727
1-NP	0.82755346	0.87071435	0.87205706	0.89781799
2-NB	0.84903690	0.91654214	0.87817329	0.90527546
2-M-1-NP	0.84062449	0.84874109	0.87663423	0.92334125
1-NB	0.15683948	0.14278754	0.98624950	0.80736793

Table 6. Analysis of variance for Equation 32 for 2-NB in the CT series

Source of Variation	Degrees of Freedom	Sum of Squares	Mean Square	F
Fitting all terms	3	0.16155412	0.053851368	
Error	54	0.030760867	0.00056964564	
Total	57	0.19231499		
Omitting β_0	3	2.5100238	0.83667455	
Error	55	0.030782110	0.0005596747	0.037
Total	58	2.5408059		

ing flow rate. These data were also fit to Equation 32 without the β_0 term by fitting the uncorrected sums of squares rather than the corrected sums of squares. Under these conditions, the multiple correlation coefficient cannot be exactly calculated. Instead, an F-test (reference 23, chapters 8 and 9) was made from the data in the analysis of variance presented in Table 6 as shown below.

$$F^{\eta_1}_{\eta_2} = \frac{\eta_2}{\eta_1}\left[\frac{\begin{pmatrix}\text{Error sum of squares without } \beta_0 - \\ \text{Error sum of squares with } \beta_0\end{pmatrix}}{\text{Expected mean square with } \beta_0}\right]$$

The results shown in Table 6 are for 2-NB in the CT series and are representative of the results obtained in this investigation. The calculated value of F^{1}_{54} is not significant. This means that the β_0 term may be omitted from the regression model without any significant decrease in accuracy.

Since this experimental work was done, Jones (17) has also modified van Deemter's original equation to include terms for the resistance to mass transfer through the stagnant gas in and surrounding each particle (β_3W_3), the effects of velocity gradients in the column (β_4W_4), and effect of a postulated interaction (β_5W_5), between the β_3W_3 and β_4W_4 terms. Jones Equation 25 is given below in model form as:

$$Y = \beta_0 + \beta_1W_1 + \beta_2W_2 + \beta_3W_3 + \beta_4W_4 + \beta_5W_5 \qquad (36)$$

where

$$\beta_0 = A \qquad (37a)$$

$$\beta_1 = B \qquad (37b)$$

$$\beta_2 = c_1 d_\ell^2 \qquad (37c)$$

$$\beta_3 = c_2 d_g^2 \qquad (37d)$$

$$\beta_4 = c_3 d_p^2 \qquad (37e)$$

$$\beta_5 = 2\rho\ (c_2 c_3)^{1/2} d_p d_h \qquad (37f)$$

β_0, $\beta_1 W_1$, and $\beta_2 W_2$ correspond to the A, B, and C terms of the original van Deemter equation.

Using Equation 26 and making the change from linear to volumetric flow rates the W_i can be written as:

$$W_1 = T^{3/2}/F \qquad (38a)$$

$$W_2 = \frac{kF}{(1+k)^2 D_\ell} \qquad (38b)$$

$$W_3 = \frac{k^2 F}{(1+k)^2 T^{3/2}} \qquad (38c)$$

$$W_4 = \frac{F}{T^{3/2}} \qquad (38d)$$

$$W_5 = \frac{kF}{(1+k)T^{3/2}} \qquad (38e)$$

The experimental data obtained in this study were also correlated by multiple linear regression using Equation 36 as the model. When all six terms of the Jones equation were used for the correlation, the results are as shown in Table 20. The code numbers 1, 2, 3, 4, in Table 20 indicate the multiple regression analysis of the CT + LTP, CT, LTP, and RFTP data. The corresponding values of R are shown in Table 7. The absence of a regression equation for any compound under any one of these four methods of analysis indicates that some of the W_i terms were so closely correlated that the correlation matrix became singular and thus could not be inverted.

Following the suggestions of Jones (17), Giddings and Robison (14) and van Deemter _et_ _al_. (9) that the term corresponding to $\beta_3 W_3$ is not greatly significant with respect to the other terms in Equation 36 the experimental data were fitted to Equation 36 without the $\beta_3 W_3$ term. The regression coefficients are shown in Table 8. Although the values in Table 8 corresponding to those in Table 7 differ by less than 1 percent, the omission of the $\beta_3 W_3$ term allows the inversion of the S matrix. This means that if the $\beta_3 W_3$ is omitted, the data can be significantly correlated and Giddings earlier suggestion (11) of a trivial $\beta_3 W_3$ for packed columns is verified for this data. This in turn leads to the

Table 7. Values of R for the fit of Equation 36

Compound	LTP + CT	CT	LTP	RFTP
NM	----	0.43975976	----	----
NE	0.81588971	0.51420492	----	----
2-NP	----	----	----	0.93795465
2-M-2-NP	0.84132211	0.80023835	0.87279937	0.93273152
1-NP	0.84871020	----	----	0.90219875
2-NB	----	0.86744177	----	----
2-M-1-NP	----	----	----	0.94403234
1-NB	----	----	----	----

Table 8. Values of R for the fitting of Equation 36 without $\beta_3 W_3$

Compound	LTP + CT	CT	LTP	RFTP
NM	0.65959837	0.43988938	0.73124851	0.28032044
NE	0.81733209	0.51245387	0.86438251	0.86689553
2-NP	0.84054698	0.83845427	0.87736759	0.93784971
2-M-2-NP	0.83821981	0.79777269	0.86541003	0.93242303
1-NP	0.84890948	0.35144867	0.87974733	0.90188418
2-NB	0.84134451	0.85893614	0.89173630	0.91545262
2-M-1-NP	0.85741741	0.81437049	0.88812136	0.94372739
1-NB	0.18208811	0.17047797	0.98655336	0.85765922

conclusion that the eddy diffusion concept in gas chromatography theory is incorrect.

Further evidence is found in the analysis of variance for Equation 36. Representative data are shown for 2-NB in the CT series. To test whether or not a given $\beta_i W_i$ term is significant, that term is omitted from the regression model and the data are fitted to the reduced model. The significance of the $\beta_i W_i$ term is then tested by an F-test as shown below.

$$F^{\eta_1}_{\eta_2} = \frac{\eta_2}{\eta_1}\left[\frac{R^2 \text{ for full model} - R^2 \text{ for reduced model}}{1 - R^2 \text{ for full model}}\right]$$

The calculated values of F were compared with $F^{\eta_1}_{\eta_2}$ (0.05). If the calculated value of F was less than the tabular value of F for the corresponding degrees of freedom, then the associated $\beta_i W_i$ term does not contribute significantly to the regression model and may be deleted. From the analysis of variance for Equation 36 presented in Table 9, $\beta_3 W_3$ is clearly insignificant.

A further analysis of the experimental data was made using Equation 36 without the $\beta_3 W_3$ and $\beta_5 W_5$ terms (omitting the contributions of stagnant gaseous diffusional resistance and the interaction terms, respectively). The resulting regression coefficients are shown in Tables 29 to 32 with the corresponding R values shown in Table 10. On comparing the R values in Table 10 with those in Table 8, it is evident

Table 9. Analysis of variance for Equation 36 for 2-NB in the CT series

Source of Variation	Degrees of Freedom	Sum of Squares	Mean Square	F	R^2
Fitting all terms	5	0.14470843	0.02894168		0.75245523
Error	52	0.047606555	0.00091551062		
Total	57	0.19231499			
Omitting β_3W_3	4	0.14188449	0.03547118		0.73777130
Error	53	0.050430500	0.00095151882	0.074	
Total	57	0.19231499			
Omitting β_3W_3 and β_4W_4	3	0.099880790	0.033293596		0.51936039
Error	54	0.092434200	0.0017117444	1.110	
Total	57	0.19231499			
Omitting β_3W_3 and β_4W_4	3	0.10020547	0.033401818		0.52104862
Error	54	0.092109520	0.0017057318	1.102	
Total	57	0.19231499			
Omitting β_0, β_3,W_3, and β_4W_4	3	2.4474160	0.81580528		
Error	55	0.093389900	0.0016981800	0.558	
Total	58	2.5418059			

Table 10. Values of R for the fitting of Equation 36 without β_3W_3 and β_5W_5

Compound	LTP + CT	CT	LTP	RFTP
NM	0.21004036	0.40536616	0.72390802	0.27987972
NE	0.76292934	0.46662840	0.84327797	0.86518022
2-NP	0.83628454	0.72888997	0.83965514	0.93472936
2-M-2-NP	0.68969111	0.62849884	0.85957593	0.92902882
1-NP	0.80561465	0.34192771	0.84989245	0.90148073
2-NB	0.59566321	0.72183697	0.89137464	0.91538330
2-M-1-NP	0.58424964	0.59745059	0.87869004	0.94369915
1-NB	0.12037517	0.14207388	0.98619419	0.81513681

that the contribution of the β_5W_5 term can probably be safely ignored as the R values in Table 10 are only a few hundredths lower than the corresponding R values in Table 8. Further evidence for this was found by fitting Equation 36 without the β_3W_3 and β_4W_4 terms. The regression coefficients are shown in Tables 33 to 36. The corresponding values of R are shown in Table 11. By comparing the R values of Table 10 where Equation 36 was fitted without the β_3W_3 and the β_5W_5 terms with the R values of Table 11 where Equation 36 was fitted without the β_3W_3 and the β_4W_4 terms, it is seen that corresponding R values are almost identical. This would seem to bear out the suggestion of Giddings and Robison (14) that neither these terms, β_4W_4 and β_5W_5, are of major significance in the explanation of the chromatographic mechanism.

When the data of Tables 8, 10, and 11 are examined entry by entry, it is seen that the values of R change very little whether the β_4W_4 and β_5W_5 terms are omitted or not. This is further evidence that the concept of eddy gas phase diffusion term proposed by van Deemter _et al_. (9) is in error as suggested by Giddings (12, 13). This also strengthens the conclusion that the primary resistances to mass transfer is the gas chromatographic process are molecular diffusion in the gas phase and the diffusion of the solutes in the liquid phase.

The non-significance of the $\beta_4 W_4$ and $\beta_5 W_5$ terms is also demonstrated by their corresponding F-tests as shown in Table 9.

The significance of β_0 in Jones' equation can be tested by comparing the error sum of squares resulting from fitting Equation 36 without β_0, $\beta_3 W_3$, and $\beta_4 W_4$ to that resulting from fitting Equation 36 without $\beta_3 W_3$ and $\beta_4 W_4$. As seen in Table 9, the resulting F-test shows that β_0 is not significant.

Table 11. Values of R for the fitting of Equation 36 without the $\beta_3 W_3$ and $\beta_4 W_4$ terms

Compound	LTP + CT	CT	LTP	RFTP
NM	0.21484721	0.40468942	0.72386921	0.27892478
NE	0.76377235	0.46680279	0.84322380	0.86517798
2-NP	0.83647269	0.72809024	0.83965581	0.93455712
2-M-2-NP	0.69039409	0.62630440	0.85963930	0.92832493
1-NP	0.80616630	0.34185044	0.84987783	0.90160489
2-NB	0.59642018	0.72066662	0.89136080	0.91529018
2-M-1-NP	0.58489681	0.59604672	0.87861388	0.94360122
1-NB	0.12055353	0.14213089	0.98619595	0.81058145

DISCUSSION OF RESULTS

On the basis of the different R values resulting from this work when the experimental data were fit to the equations derived by Bethea and Adams (3) and Jones (17), it is concluded that for those data, the A term in van Deemter's equation has no physical significance and that either equation is equally as good for the explanation of these data. It is also concluded that Jones' addition of a correction term to account for differences in gas phase residence times is not significant.

Observed values of HETP ranged from 0.1 to 0.35 cm. for the CT series, from 0.04 to 0.27 cm. for the LTP series, and from 0.09 to 0.33 cm. for the RFTP series. When the values of HETP are plotted against carrier gas flow rate, F, it is seen that the curves show minimum values at a hydrogen flow rate between 90 and 120 ml./min. Representative data are shown in Figure 6 for 2-NB in the CT series where levels of constant temperature operation have been used as the parameter. Also shown are curves corresponding to fitting Equation 32 without β_0 (solid line) and Equation 36 without the β_0 and $\beta_3 W_3$ terms (dotted line). These curves represent the values calculated for HETP when the β_i values shown in

Tables 17 and 26 were used. These models represent the best fits obtained by the regression programs as measured by the multiple correlation coefficient. Comparing the experimental data to the HETP values calculated from the equations obtained by fitting these simplified equations of these equations presents the significant aspects of this investigation in an easily comparable form. It is obvious that both of these models are equally effective in correlating the experimental data.

Temperature Effects

Values for HETP are greatly influenced by temperature. As seen in Figure 6, HETP values at any flow rate remain approximately the same as the temperature is raised from 40 to 50°C but then almost double as the temperature is increased to 80°C. This can be partly explained by considering HETP as defined by Equation 27. At any flow rate, as the temperature is increased in discrete steps, term 2 of Equation 27 increases and terms 3, 4, and 5 decrease. This would be expected as molecular diffusion in the liquid phase is directly proportional to the absolute temperature and inversely proportional to the viscosity whereas the molecular diffusion in the gas phase is directly proportional to $T^{3/2}$.

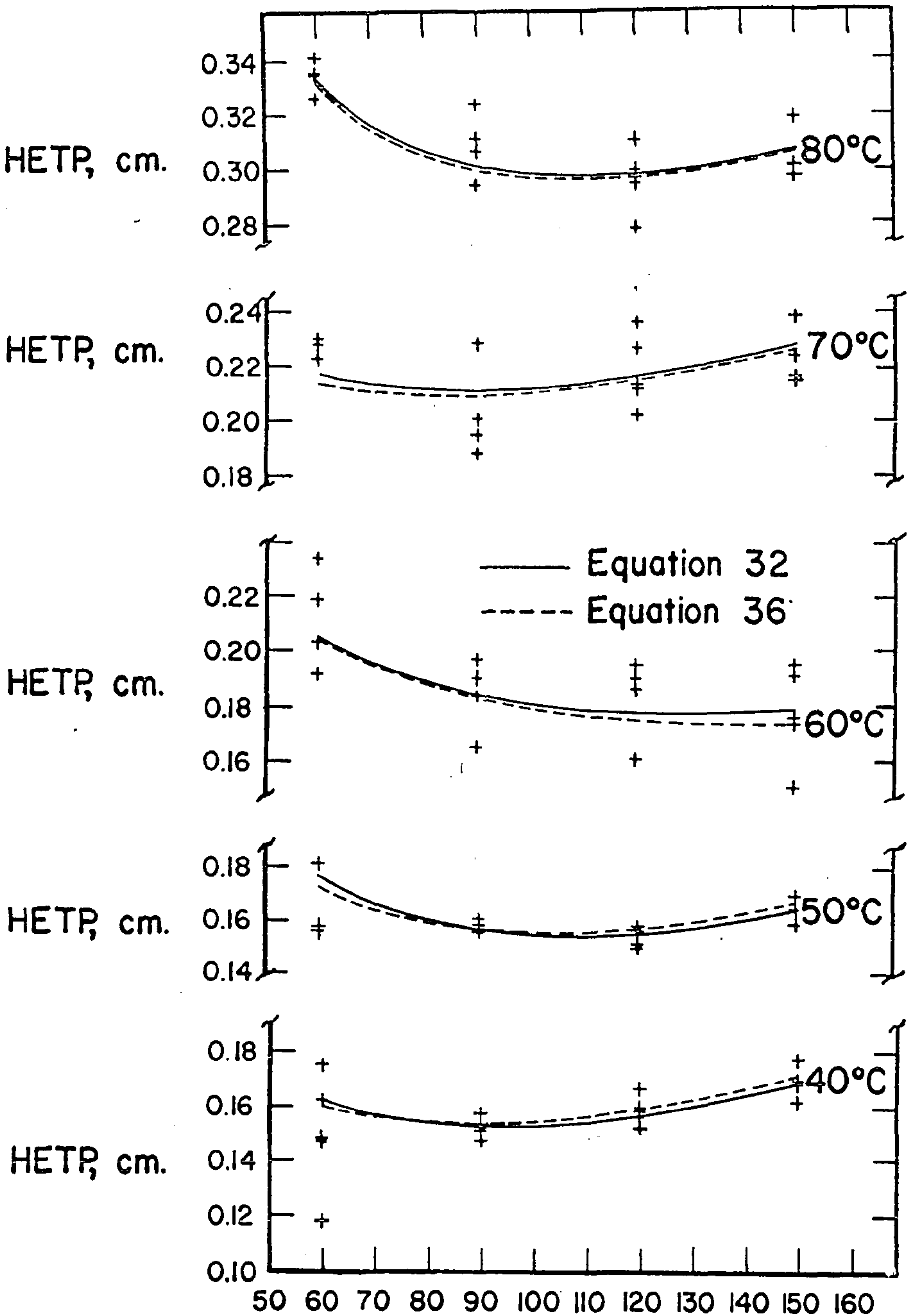

Figure 6. Comparison of experimental with predicted values of HETP for the CT series for 2-NB

The change in d_ℓ due to thermal expansion of the substrate should be minor. The same may be said of d_h and ℓ. The particle diameter, d_p, will be even less affected by thermal expansion.

If diffusion in the liquid phase were the controlling factor in the chromatographic process, then θ_i^2 would increase with increasing temperature as T/e^T. As it is well known that θ_i decreases with increasing temperature and if the first term of Equation 27 does not change with temperature or flow rate, the rate controlling step in this case must not be diffusion in the liquid phase. As temperature increases, term 2 of Equation 27 increases as $T^{3/2}$ and terms 3 and 4 decrease as $T^{3/2}$. So the net effect of a temperature increase is to increase term 2 while all other terms remain constant or decrease. This clearly indicates the importance of molecular diffusion in the chromatographic separation process.

Changes in the right hand side of Equation 27 cannot be said to influence only θ_i as this equation shows the physical effects on $(w_i/\theta_i)^2$. It has been observed in the course of this investigation that increases in T cause a decrease in w_i but the percentage change in w_i is not as great as that in θ_i. This was especially noticeable for components eluted after 1-NP. Golay's work (16) on early peaks, primarily air (whose retention times are practically unaffected by most substrates) related changes in HETP to changes in w_i. His work was considered as evidence for modification of the van Deemter equation to account for diffusional effects in the bulk gas stream.

The dependence of θ_i on absolute temperature at constant flow rates has been adequately demonstrated (8, 22). These data may be generally represented as:

$$\theta_i = \frac{c_1 e^{c_2/T}}{F} \qquad (39)$$

Equation 39 independently permits the prediction of changes in θ_i caused by temperature changes in constant flow work. The combined use of Equations 27 and 39 may make it possible in the future to predict separately the effect of temperature on solute band width, w_i. This presupposes exact knowledge of the dependence of k on temperature. Unfortunately, such data are at present available for only three or four chromatographic systems.

Values of k, the partition ratio, for this work ranged for 293.4 at 80°C and 60 ml. H_2/min. to 1602.4 at 40°C and

150 ml. H_2/min. and decreased with increasing temperatures as the flow rate was held constant. The changes in k with temperature as a constant flow rate provide an additional decrease in the denominators of terms 3, 4, and 5 of Equation 27, thus decreasing θ_i if any of these terms were the rate-controlling step. As k also appears in the numerator of term 5, the effect of liquid phase diffusion on θ_i would be expected to decrease with increasing temperature. This is a logical assumption since it is well known that the rate of solute diffusion in Newtonian liquids increases with temperature, i.e. the kinetic energy of both the substrate and solute molecules increases (reference 25, pp. 21-24).

Flow Rate Effects

For a constant mass of solute added, the primary effect of a flow rate increase at a constant temperature is a decrease in retention time. An increase in flow rate will decrease the mass transfer rate in the bulk gas phase because of the impeding effect of an increased number of carrier gas molecules in the bulk gas phase, i.e., the solute concentration in the bulk gas phase becomes more dilute with a corresponding decrease in concentration gradient from the gas phase to the liquid phase. As F increases at a constant value of R_h the terms where the influence of temperature predominates should increase in proportion to the length of time that a particular component is exposed to the higher temperatures. The temperature effects in terms 2, 3, 4, and 5 of Equation 27 oppose the flow rate effect to some extent. As temperature appears as $T^{3/2}$ in terms 2, 3, and 4 and as $e^T/T^{1/2}$ in term 5, and F appears in all four terms only as the first power, the effect of temperature increases by linear programming should gradually become more apparent as F/R_h increases. Flow rate has little effect on k. A flow rate increase has the effect of decreasing term 2 of Equation 27 with a corresponding increase in θ_i and a decrease in w_i if molecular diffusion in the bulk gas stream is the rate-controlling process. This does not happen. A flow rate increase will directly increase terms 3, 4, and 5 with a corresponding decrease in θ_i which is known to occur. The controlling rate process then is a combination of one or more of terms 3, 4, and 5 of Equation 27, i.e., the rate of mass transfer.

At this point the reader may raise the question: Why not disregard term 4 of Equation 27 and include in term 3 the resistance to mass transfer in the stagnant gas-filled pores? This simplification would be possible if only a single standard support were universally used. Baker et al. (2) have demonstrated that both the number and the pore size distribution change with type of support material. Zlatkis, Ling, and Kaufman (27) have shown that chemical pretreatment has an effect on the retention time at least partially due to structural changes in the support. These changes are reflected in d_h which appears in term 4. Experiments in this laboratory, which were identical except for chemical pretreatment of the brick, have shown differences in both θ_i and w_i (and thus, H) which are most easily explained by inclusion of a term such as term 4.

BIBLIOGRAPHY

1. Adams, F. S. Vapor phase nitration of butane in a fused salt reactor. Unpublished Ph.D. thesis. Ames, Iowa, Library, Iowa State University of Science and Technology. 1961.

2. Baker, W. J., Lee, E. H., and Wall, R. F. Chromatographic solid support studies. In Noebels, H. J., Brenner, N. and Wall, R. F., eds. Gas chromatography. pp. 21-32. New York, New York, Academic Press, Inc. 1961.

3. Bethea, R. M. and Adams, F. S. Gas chromatography of the C_1 to C_4 nitroparaffins: isothermal vs. linear temperature programming. Anal. Chem. 33: 832-839. 1961.

4. ________ and ________. Vapor phase butane nitration: product analysis by parallel column gas chromatography. J. Chromatog. 10: 1-8. 1963.

5. Bohemen, J. and Purnell, J. H. Some applications of theory in the attainment of high column efficiencies in gas-liquid chromatography. In Desty, D. H., ed. Gas chromatography 1958. pp. 23-35. London, England, Butterworths Scientific Publications. 1958.

6. ________ and ________. Diffusional band spreading in gas-chromatographic columns. I. The elution of unsorbed gases. J. Chem. Soc. 1961: 360-367. 1961.

7. ________ and ________. Diffusional band spreading in gas chromatographic columns. II. The elution of sorbed vapours. J. Chem. Soc. 1961: 2630-2638. 1961.

8. Dal Nogare, S. and Juvet, R. S. Gas-liquid chromatography: theory and practice. New York, New York, John Wiley and Sons. 1962.

9. Deemter, J. J. van, Zuiderweg, F. J., and Klinkenberg, A. Longitudinal diffusion and resistance to mass transfer as causes of nonideality in chromatography. Chem. Eng. Sci. 5: 271-289. 1956.

10. Ergun, S. Fluid flow through packed columns. Chem. Eng. Prog. 48: 89-94. 1952.

11. Giddings, J. C. Nature of gas phase mass transfer in gas chromatography. Anal. Chem. 34: 1186-1192. 1962.

12. ________. Plate height of nonuniform chromatographic columns; gas compression effects, coupled columns, and analogous systems. Anal. Chem. 35: 353-356. 1963.

13. ________. Evidence on the nature of eddy diffusion in gas chromatography from inert (nonsorbing) column data. Anal. Chem. 35: 1338-1341. 1963.

14. ________ and Robison, R. A. Failure of the eddy diffusion concept of gas chromatography. Anal. Chem. 34: 885-890. 1962.

15. Glueckauf, E. Theory of chromatography. IX. The "theoretical plate" concept in column separations. Faraday Soc. Trans. 51: 34-44. 1955.

16. Golay, M. J. E. Theory of chromatography in open end coated tubular columns with round and rectangular cross sections. In Desty, D. H., ed. Gas chromatography 1958. pp. 36-55. London, England, Butterworths Scientific Publications. 1958.

17. Jones, W. L. Modifications to the van Deemter equation for the height equivalent to a theoretical plate in gas chromatography. Anal. Chem. 33: 829-832. 1961.

18. ________ and Kieselbach, R. Units of measurement in gas chromatography. Anal. Chem. 30: 1590-1592. 1958.

19. Keulemans, A. I. M. Gas chromatography. 2nd ed. New York, New York, Reinhold Publishing Corp. 1959.

20. Kieselbach, R. Gas chromatography; source of the velocity independent A term in the van Deemter equation. Anal. Chem. 33: 806-807. 1961.

21. Klinkenberg, A. and Sjenitzer, F. Holding-time distributions of the Gaussian type. Chem. Eng. Sci. 5: 258-270. 1956.

22. Littlewood, A. B. Gas chromatography: principles, techniques, and applications. New York, New York, Academic Press, Inc. 1962.

23. Ostle, B. Statistics in research. 2nd ed. Ames, Iowa, Iowa State University Press. 1963.

24. Perrett, R. H. and Purnell, J. H. Contribution of diffusion and mass transfer processes to efficiency of gas liquid chromatography columns. Anal. Chem. 35: 430-439. 1963.

25. Treybal, R. E. Mass transfer operations. New York, New York, McGraw-Hill Publishing Company, Inc. 1955.

26. Wilke, C. R. and Chang, P. Correlation of diffusion coefficients in dilute solutions. A. I. Ch. E. Journal 1: 264-270. 1955.

27. Zlatkis, A., Ling, S., and Kaufman, H. R. Resolution of isomeric xylenes by gas chromatography. Anal. Chem. 31: 945-947. 1959.

ACKNOWLEDGMENTS

The author wishes to express his appreciation to Dr. Morton Smutz for his help, encouragement, and constructive criticism during this investigation.

Appreciation is also due Dr. George Burnet and Dr. D. R. Boylan for providing the equipment and supplies used through the facilities of the Chemical Engineering Department and the Iowa Engineering Experiment Station; to Mr. John H. Bolton for patient review and assistance with the preparation of scientific articles resulting from this work; to Mr. Walter Kolpin for assistance with construction and repairs of various parts of the apparatus; and to the other members of the Chemical Engineering Department, past and present, whose cooperation and assistance furthered the progress of this work.

Grateful appreciation is extended to Dr. Frank S. Adams, Jr., without whose assistance in obtaining and interpreting the data this work would not have been completed.

Last, but by no means least, the author wishes to thank his wife, Nancy Jo Bethea, for patiently enduring the trying periods during his preliminary examinations and the preparation of this dissertation.

Part of the material in this dissertation has been taken from Analytical Chemistry, Vol. 33, pages 832-839, 1961, copyright 1961, by the American Chemical Society and has been reproduced by permission of the copyright owner.

APPENDIX

Table 12. Regression coefficients from fitting LTP + CT data to Equation 32

Compound	Coefficients			
	$\beta_0(10^2)$	$\beta_1(10^4)$	$\beta_2(10^{-4})$	$\beta_3(10^8)$
NM	4.444308	5.726497	6.853421	2.6327028
NE	6.818372	1.096863	7.2775848	7.016418
2-NP	5.78631	2.088809	4.890463	12.148285
2-M-2-NP	0.111599	3.059022	28.382413	0.110169726
1-NP	38.7704	3.062711	18.997769	0.12586931
2-NB	-6.120201	7.799626	157.17741	0.29752865
2-M-1-NP	-4.467527	4.893673	116.42002	0.21380978
1-NB	-2.430241	-12.19713	735.37819	0.98544825

Table 13. Regression coefficients from fitting CT data to Equation 32

Compound	Coefficients			
	$\beta_0(10^2)$	$\beta_1(10^4)$	$\beta_2(10^{-4})$	$\beta_3(10^8)$
NM	18.840216	0.4529062	3.1131077	-0.71788524
NE	20.14645	-3.1353477	-1.5320212	0.45878374
2-NP	20.723033	-1.468639	-11.6764	0.14177825
2-M-2-NP	5.828056	4.3225995	1.6705089	2.9963601
1-NP	7.917466	3.1337102	3.331396	2.5486421
2-NB	0.673914	13.364982	134.84438	9.5808024
2-M-1-NP	-3.9319320	10.774274	111.336066	0.111762691
1-NB	0.014407106	-109.28736	307.1789	-196.28

Table 14. Regression coefficients from fitting LTP data to Equation 32

Compound	Coefficients			
	$\beta_0(10^2)$	$\beta_1(10^4)$	$\beta_2(10^{-4})$	$\beta_3(10^8)$
NM	6.80973	2.107126	2.6524257	3.3797932
NE	11.579678	-3.3166306	-13.720144	7.4654334
2-NP	11.572386	-3.31194	-32.58913	12.703878
2-M-2-NP	4.436526	-0.840491	-10.79296	10.934006
1-NP	4.43461	-0.624879	-22.120582	11.989731
2-NB	1.892611	1.533205	22.230335	25.778222
2-M-1-NP	0.392514	1.18163	26.57855	18.69793
1-NB	1.159122	0.3087454	-5.217097	33.396306

Table 15. Regression coefficients from fitting RFTP data to Equation 32

Compound	Coefficient			
	$\beta_0(10^2)$	$\beta_1(10^3)$	$\beta_2(10^{-4})$	$\beta_3(10^8)$
NM	-6.71855	2.039391	-2.999976	2.0267807
NE	84.615007	-7.1800395	4.7837841	0.26968153
2-NP	89.295722	-7.6343297	19.231872	0.44536785
2-M-2-NP	32.421082	-2.6129454	-2.05771	2.0064146
1-NP	15.686721	-0.9782327	-36.03093	6.5606357
2-NB	25.29013	-1.979123	23.7282	12.170274
2-M-1-NP	10.586679	-7.713533	7.388525	8.3014252
1-NB	16.875166	-1.3026438	4.8338807	-9.5854141

Table 16. Regression coefficients from fitting LTP + CT data to Equation 32 without the β_0 term

Compound	Coefficients		
	$\beta_1(10^5)$	$\beta_2(10^7)$	$\beta_3(10^7)$
NM	93.806050	0.07501739	34.978613
NE	71.034050	0.09775428	94.739328
2-NP	72.382430	0.08704260	148.24892
2-M-2-NP	31.578200	0.28505290	102.32730
1-NP	34.072600	0.19513350	128.44865
2-NB	25.237690	1.4071182	241.91310
2-M-1-NP	10.445010	1.0325414	169.01153
1-NB	-141.74106	7.2037501	945.36059

Table 17. Regression coefficients from fitting CT data to Equation 32 without the β_0 term

Compound	Coefficients		
	$\beta_1(10^5)$	$\beta_2(10^7)$	$\beta_3(10^7)$
NM	128.00954	0.068380347	26.628629
NE	102.06410	0.082936934	78.626891
2-NP	124.09067	0.046184980	117.09960
2-M-2-NP	82.361630	0.23608074	66.688002
1-NP	84.609560	0.14298493	85.932850
2-NB	138.21349	1.3646255	102.99144
2-M-1-NP	80.927900	1.0327006	71.237358
1-NB	107.34929	9.8442190	780.32587

Table 18. Regression coefficients from fitting Equation 32 without the β_0 term

Compound	Coefficients		
	$\beta_1 (10^5)$	$\beta_2 (10^7)$	$\beta_3 (10^7)$
NM	76.605415	0.05636537	47.210911
NE	58.635000	0.04917370	125.77850
2-NP	55.637140	0.00237850	198.55062
2-M-2-NP	24.571460	0.07512910	146.24778
1-NP	27.243864	0.01475080	166.77236
2-NB	29.393522	0.35116590	287.15004
2-M-1-NP	14.761532	0.29360690	193.88163
1-NB	11.952613	0.05487775	367.00147

Table 19. Regression coefficients from fitting Equation 32 without the β_0 term

Compound	Coefficients		
	$\beta_1(10^5)$	$\beta_2(10^7)$	$\beta_3(10^7)$
NM	135.37128	-0.02339229	18.150003
NE	131.32548	-0.36708575	64.951214
2-NP	132.22622	-0.77907800	112.12633
2-M-2-NP	64.064024	-0.64684183	72.904461
1-NP	58.437332	-0.76926232	96.972159
2-NB	46.030190	-0.79791660	203.65075
2-M-1-NP	23.390970	-0.39508890	124.28432
1-NB	13.153853	-0.29201251	205.13070

Table 20. Regression coefficients from fitting all data to Equation 36

Compound	Code	Coefficients					
		$\beta_0(10^5)$	$\beta_1(10^5)$	$\beta_2(10^7)$	β_3	β_4	β_5
NE	1	18669.637	68.945856	0.73561462	1684.3450	1099.7558	2779.1213
2-M-2-NP	1	8612.9299	25.032698	1.0944800	876.05608	587.63031	283.78914
1-NP	1	415535.357	67.238172	1.3736305	65.965200	900.45136	972.55065
2-NP	4	429580.90	1579.6801	0.60916030	7273.9900	10779.950	17773.729
2-M-2-NP	4	440376.27	1849.9007	0.59967939	4195.3630	6312.3930	10247.227
1-NP	4	169303.92	715.99406	0.24191598	3766.5461	3144.5397	6806.1099
2-M-1-NP	4	182655.06	763.24618	0.09462422	3479.7742	3695.7941	7064.4466
NM	2	15402.417	29.777436	0.06022574	156.07116	326.32023	170.95868
NE	2	16962.875	6.1180222	0.12412532	388.94572	50.020050	435.91631
2-NP	2	275.84075	82.519038	0.33530237	564.36007	379.94105	184.94200
2-NB	2	9455.5758	208.68601	1.0419527	1594.1371	3007.8138	1413.9089
2-M-2-NP	3	634.97319	25.659050	1.0081156	788.36320	5.0000100	790.56255

Table 21. Regression coefficients from fitting LTP + CT data to Equation 36 without the $\beta_3 W_3$ term

Compound	Coefficients				
	$\beta_0 (10^5)$	$\beta_1 (10^5)$	$\beta_2 (10^7)$	β_4	β_5
NM	8394.8040	29.516202	0.27500642	988.81236	-993.23045
NE	18594.802	-68.652524	0.73469503	582.26013	-587.22335
2-NP	22888.604	-92.432758	1.2741629	257.24946	-263.37406
2-M-2-NP	8680.0320	-25.203735	1.0922562	1425.5379	-1430.1268
1-NP	14528.432	-67.220621	1.3738680	838.76390	-844.90256
2-NB	16899.425	-64.549458	3.4506659	5390.9399	-5403.6135
2-M-1-NP	9291.7110	-37.661750	2.5483820	4207.0861	-4215.5689
1-NB	78453.689	-612.54008	13.890395	20996.541	-21040.962

Table 22. Regression coefficients from fitting CT data to Equation 36 without the $\beta_3 W_3$ term

Compound	Coefficients				
	$\beta_0(10^5)$	$\beta_1(10^5)$	$\beta_2(10^7)$	β_4	β_5
NM	15408.488	29.699590	-0.05977644	481.10515	-481.82081
NE	16941.380	-6.1214089	-0.11596312	-324.27730	327.23673
2-NP	21369.285	-17.336929	-0.09847050	-1034.3018	1037.0216
2-M-2-NP	295.31259	82.562065	0.32057089	923.56483	-922.95285
1-NP	8164.2285	30.184640	0.22967263	114.51923	-114.59840
2-NB	-9451.3065	210.44032	0.75424100	5314.6493	-4313.8392
2-M-1-NP	-7668.3267	134.32163	0.9160580	4126.2417	-4129.6482
1-NB	255035.23	-1969.7160	17.111740	29932.807	-30040.336

Table 23. Regression coefficients from fitting LTP data to Equation 36 without the β_3W_3 term

Compound	Coefficients				
	$\beta_0(10^5)$	$\beta_1(10^5)$	$\beta_2(10^7)$	β_4	β_5
NM	5922.7914	27.199424	0.33802102	248.35123	-248.63967
NE	13217.597	-44.075515	0.74877180	-819.09566	819.72574
2-NP	10159.738	-25.686723	1.2214211	-1486.6543	1488.8763
2-M-2-NP	-931.12460	23.739503	0.98478717	-344.76269	347.04735
1-NP	4102.8075	-9.4048110	1.2211838	-1025.0829	1025.8352
2-NB	-8041.8431	78.393753	2.2052605	211.37064	-207.58621
2-M-1-NP	-6802.5523	55.711234	1.5733776	689.74137	-687.44444
1-NB	33.212098	7.7205189	3.2746928	-145.50770	145.92857

Table 24. Regression coefficients from fitting RFTP data to Equation 36 without the $\beta_3 W_3$ term

Compound	Coefficients				
	$\beta_0(10^5)$	$\beta_1(10^5)$	$\beta_2(10^7)$	β_4	β_5
NM	1822792.8	-9402.1203	0.22592536	-1382.3427	513.34675
NE	-207525.60	625.84450	-0.26416820	1512.8290	-1357.9222
2-NP	-427333.70	1571.5623	-0.59830410	3513.3900	-3234.6505
2-M-2-NP	-442657.36	1858.9170	-0.60679080	2192.3220	-1930.5159
1-NP	-167581.43	708.55887	0.24524021	-592.44180	696.48897
2-NB	-292070.53	1210.3174	0.29258956	513.03490	-334.05231
2-M-1-NP	-180109.74	752.45940	0.08927711	207.20325	-97.568389
1-NB	-130471.82	467.42103	-2.6151098	1661.3720	-1571.6527

Table 25. Regression coefficients from fitting LTP + CT data to Equation 36 without the β_0 and $\beta_3 W_3$ terms

Compound	Coefficients			
	$\beta_1 (10^5)$	$\beta_2 (10^7)$	β_4	β_5
NM	88.846480	0.27980970	1021.0032	-1023.0514
NE	59.683903	0.73619381	617.95920	-617.14286
2-NP	62.837751	1.2657078	311.54753	-310.41475
2-M-2-NP	36.694692	1.0567150	976.65430	-977.53388
1-NP	37.361115	1.3359224	665.54428	-665.24528
2-NB	----	----	----	----
2-M-1-NP	33.001890	2.2919510	2462.0888	-2465.1722
1-NB	-59.956088	10.317560	9210.2035	-9215.3782

Table 26. Regression coefficients from fitting CT data to Equation 36 without the β_0 and $\beta_3 W_3$ terms

Compound	Coefficients			
	$\beta_1 (10^5)$	$\beta_2 (10^7)$	β_4	β_5
NM	138.56776	-0.06689938	494.08245	-489.92248
NE	113.83010	-0.14330951	-317.48434	325.93407
2-NP	133.75362	-0.13587210	-1008.9116	1018.4745
2-M-2-NP	87.360372	0.089043320	643.88321	-641.72414
1-NP	88.147469	0.18260913	102.01155	-99.347826
2-NB	141.58949	1.1068320	4606.1575	-4609.5238
2-M-1-NP	81.249570	1.7121090	3892.6279	-3897.7251
1-NB	140.16825	9.2579400	26377.155	-26391.044

Table 27. Regression coefficients from fitting LTP data to Equation 36 without the β_0 and $\beta_3 W_3$ terms

Compound	Coefficients			
	$\beta_1(10^5)$	$\beta_2(10^7)$	β_4	β_5
NM	69.090838	0.33781652	297.96573	-296.66666
NE	41.868117	0.68789661	495.45505	-499.73684
2-NP	47.550439	1.1809291	-2218.9785	2225.9090
2-M-2-NP	20.556371	1.0104688	-660.22648	662.63158
1-NP	----	----	----	----
2-NB	30.870420	2.4359401	45.988536	-45.000000
2-M-1-NB	16.667840	1.7897926	432.10660	-432.08333
1-NB	9.3437430	3.2617251	-99.130889	99.642857

Table 28. Regression coefficients from fitting RFTP data to Equation 36 without the β_0 and $\beta_3 W_3$ terms

Compound	Coefficients			
	$\beta_1 (10^5)$	$\beta_2 (10^7)$	β_4	β_5
NM	21.182667	0.10583543	25.155070	-14.231977
NE	----	----	----	----
2-NP	----	----	----	----
2-M-2-NP	-117.56479	0.14166908	-3.1414700	21.367144
1-NP	----	----	----	----
2-NB	----	----	----	----
2-M-1-NP	----	----	----	----
1-NB	-40.905146	-0.40980171	350.09310	-342.53659

Table 29. Regression coefficients from fitting LTP + CT data to Equation 36 without the $\beta_3 W_3$ and $\beta_5 W_5$ terms

Compound	Coefficients			
	$\beta_0 (10^5)$	$\beta_1 (10^5)$	$\beta_2 (10^7)$	β_4
NM	21858.661	-45.756450	0.14004415	-2.3319497
NE	42222.7542	-86.411920	0.70700459	-4.3484352
2-NP	23904.464	-96.801080	1.2627433	-5.8421954
2-M-2-NP	12246.196	-37.550020	1.0126839	-3.0031660
1-NP	17081.109	-71.132520	1.3238751	-5.2292706
2-NB	21234.204	-59.707820	2.8661138	-6.8205744
2-M-1-NP	11028.128	-29.546780	2.0381295	-3.9964230
1-NB	79882.370	-517.62430	8.8896108	-24.078672

Table 30. Regression coefficients from fitting CT data to Equation 36 without the $\beta_3 W_3$ and $\beta_5 W_5$ terms

Compound	Coefficient			
	$\beta_0 (10^5)$	$\beta_1 (10^5)$	$\beta_2 (10^7)$	β_4
NM	17450.396	28.109100	-0.30557656	4.5064289
NE	16377.382	-7.6613850	0.11536478	0.57520676
2-NP	20512.187	-23.826610	0.70929261	-3.5154181
2-M-2-NP	718.02500	88.452350	-0.43568375	5.2387013
1-NP	8195.2847	30.998747	0.12285191	0.45757453
2-NB	-9873.2000	241.26270	-3.6132580	16.751419
2-M-1-NP	-7982.1800	161.99440	-2.5837027	11.278289
1-NB	251145.01	-1808.3395	-23.050983	-27.219844

Table 31. Regression coefficients from fitting LTP data to Equation 36 without the β_3W_3 and β_5W_5 terms

Compound	Coefficient			
	$\beta_0(10^5)$	$\beta_1(10^5)$	$\beta_2(10^7)$	β_4
NM	6246.4954	27.524147	0.33788295	0.66071000
NE	12893.641	-50.007050	0.71636886	-1.0481682
2-NP	9316.5878	-33.961897	1.1419166	-0.00379508
2-M-2-NP	-1110.0370	22.235400	0.96630100	1.8769826
1-NP	4334.6621	-13.399413	1.1617284	-0.25273809
2-NB	-7867.5330	78.904830	2.2106847	3.9337826
2-M-1-NP	-6221.5930	57.312980	1.5828643	2.7549161
1-NB	198.07150	7.5649590	3.2865933	0.35670109

Table 32. Regression coefficients from fitting RFTP data to Equation 36 without the β_3W_3 and β_5W_5 terms

Compound	Coefficient			
	$\beta_0(10^5)$	$\beta_1(10^5)$	$\beta_2(10^7)$	β_4
NM	1360418.8	-7138.4870	0.11277102	-634.96466
NE	67152.197	-592.52951	0.03447813	5.0452557
2-NP	-109044.09	256.74156	0.09788972	96.97025
2-M-2-NP	-335923.00	1448.0434	-0.21573580	198.55988
1-NP	-191590.80	793.21780	0.10961670	118.85512
2-NB	-291915.20	1217.7567	0.34195690	178.37971
2-M-1-NP	-179662.00	752.62790	0.12561600	109.24549
1-NB	-123374.24	471.83895	-1.3698422	82.171497

Table 33. Regression coefficients from fitting LTP + CT data to Equation 36 without the $\beta_3 W_3$ and $\beta_4 W_4$ terms

Compound	Coefficients			
	$\beta_0 (10^5)$	$\beta_1 (10^5)$	$\beta_2 (10^7)$	β_5
NM	23404.789	-56.628170	0.14279975	-2.8586266
NE	22551.976	-88.661460	0.70804839	-4.4706868
2-NP	23972.147	-97.304410	1.2632944	-5.8791600
2-M-2-NP	12547.344	-39.545940	1.0142472	-3.1130489
1-NP	17214.755	-72.037720	1.3250074	-5.2848884
2-NB	21688.826	-62.626780	2.8711784	-6.9926322
2-M-1-NP	12211.129	-31.353350	2.0416501	-4.034446
1-NB	80698.190	-522.72080	8.9123574	-24.406799

Table 34. Regression coefficients from fitting CT data to Equation 36 without the β_3W_3 and β_5W_5 terms

Compound	Coefficient			
	$\beta_0(10^5)$	$\beta_1(10^5)$	$\beta_2(10^7)$	β_5
NM	17760.318	26.071050	-0.30721904	4.4537703
NE	16296.258	-7.0845170	0.11450636	0.60882189
2-NP	20353.639	-22.765920	0.71082982	-3.4808264
2-M-2-NP	813.55900	87.837600	-0.43904641	5.2315366
1-NP	8206.2088	30.926759	0.12256890	0.45578738
2-NB	-9631.5300	239.68760	-3.6253718	16.723908
2-M-1-NP	-7774.3200	160.61080	-2.5912018	11.241277
1-NB	252058.68	-1814.8597	-22.973557	-27.640739

Table 35. Regression coefficients from fitting LTP data to Equation 36 without the $\beta_3 W_3$ and $\beta_5 W_5$ terms

Compound	Coefficients			
	$\beta_0 (10^5)$	$\beta_1 (10^5)$	$\beta_2 (10^7)$	β_5
NM	6307.6169	27.106390	0.33806826	0.64289216
NE	12824.408	-49.563910	0.71574536	-1.0259975
2-NP	9226.7302	-33.390620	1.1407190	0.0281059
2-M-2-NP	-1191.5320	22.385030	0.96596790	1.8875985
1-NP	4301.2082	-13.196722	1.1609206	-0.24057632
2-NB	-7860.6330	78.893260	2.2109217	3.9352375
2-M-1-NP	-6206.9970	57.247310	1.5834093	2.7520269
1-NB	95.51290	7.5816350	3.2863631	0.35800594

Table 36. Regression coefficients from fitting RFTP data to Equation 36 without the β_3W_3 and β_4W_4 terms

Compound	Coefficients			
	$\beta_0(10^5)$	$\beta_1(10^5)$	$\beta_2(10^7)$	β_5
NM	811464.90	-4369.1760	0.03192849	-364.10178
NE	82684.987	-670.04489	0.03693898	-2.7421302
2-NP	-85065.080	147.36815	0.12522051	84.036236
2-M 2-NP	-318202.90	1373.9678	-0.16957950	188.45830
1-NP	-189557.80	788.13820	0.12919590	117.46384
2-NB	-290155.10	1214.3196	0.37339450	177.10627
2-1-NP	-178545.50	750.13350	0.14657910	108.45567
1-NB	-116491.14	445.34179	-1.2414244	77.803398